Progress in Polymer Science 39 (2014) 1498–1525

Contents lists available at ScienceDirect

Progress in Polymer Science

journal homepage: www.elsevier.com/locate/ppolysci

Recent advance in research on halloysite nanotubes-polymer nanocomposite

Mingxian Liu [a,*], Zhixin Jia [b], Demin Jia [b], Changren Zhou [a]

[a] Department of Materials Science and Engineering, Jinan University, Guangzhou 510632, PR China
[b] College of Materials Science and Engineering, South China University of Technology, Guangzhou 510640, PR China

ARTICLE INFO

Article history:
Available online 24 April 2014

Keywords:
Interfacial interaction
Dispersion
Reinforcing
Flame retardance
Crystallization
Biocompatibility

ABSTRACT

Halloysite nanotubes (HNTs) are novel 1D natural nanomaterials with predominantly hollow tubular nanostructures and high aspect ratios. Due to their high mechanical strength, thermal stability, biocompatibility, and abundance, HNTs have a number of exciting potential applications in polymer nanocomposites. In this article, we review the recent progress toward the development of HNTs-polymer nanocomposites, while paying particular attention to interfacial interactions of the nanocomposites. The characteristics of the HNTs relative to the formation of the polymer nanocomposites are summarized first. The covalent or non-covalent functionalization methods for HNTs and various fabrication approaches for HNTs-polymer nanocomposites are introduced afterward. Polymer nanocomposites reinforced with HNTs possess highly increased tensile and flexural strength, elastic moduli, and improved toughness. HNTs-polymer nanocomposites also exhibit elevated thermal resistance, flame retardance and unique crystallization behavior. Due to the tubular microstructure and the biocompatibility of HNTs, HNTs-polymer nanocomposites have demonstrated good drug encapsulation and sustained release abilities, gaining them extensive use as tissue engineering scaffolds and drug carriers. Finally, we summarize the characteristics of HNTs-polymer nanocomposites and predict for the development of the potential applications in high-performance composites for aircraft/automobile industries, environmental protection, and biomaterials.

Contents

1. Introduction 1500
2. Characteristics of HNTs relative to formation of polymer nanocomposites 1501
   2.1. Tubular microstructure 1501
   2.2. Relatively “hydrophobic” 1503
   2.3. Relatively low tube-tube interactions 1503
   2.4. Reinforcing 1503
   2.5. Flame retardance 1503
   2.6. Hydroxyl groups distribution 1503
   2.7. Negatively charged surfaces 1503

* Corresponding author. Tel.: +86 20 85223279; fax: +86 20 85223271.
E-mail addresses: liumx@jnu.edu.cn (M. Liu), tcrz9@jnu.edu.cn (C. Zhou).

http://dx.doi.org/10.1016/j.progpolymsci.2014.04.004
0079-6700/

2.8. Electrophilic 1503
2.9. Porosity and the surface defects 1503
2.10. Abundant deposition, easily available and cheap 1504
3. Functionalization of HNTs for polymer nanocomposite preparation 1504
3.1. Purification of HNTs 1504
3.2. Covalent functionalization 1504
3.2.1. Silane coupling 1504
3.2.2. Surface graft polymerization 1506
3.2.3. Covalently grafting phosphonic acid 1507
3.3. Non-covalent functionalization 1508
3.3.1. Non-covalent functionalization based on electron transfer interactions 1508
3.3.2. Non-covalent functionalization based on hydrogen bonding interactions 1508
3.3.3. Non-covalent functionalization based on electrostatic attraction interactions 1508
3.3.4. Intercalation of HNTs 1508
3.4. Enlargement of the lumen in HNTs or opening the inner-pores 1508
4. Main strategies for the fabrication of HNTs-polymer nanocomposites 1509
4.1. Processability 1509
4.2. Approaches for fabricating HNTs-polymer nanocomposites 1510
4.2.1. Solution processing 1510
4.2.2. Melt processing 1511
4.2.3. In situ polymerization 1511
4.2.4. Electrospinning 1511
4.2.5. Melt spinning 1512
4.2.6. LbL technique 1513
4.2.7. Electrophoretic deposition 1513
5. Properties of HNTs-polymer nanocomposites 1513
5.1. Mechanical reinforcement 1513
5.1.1. HNTs loading 1514
5.1.2. Dispersion 1516
5.1.3. Interfacial bonding 1516
5.2. Thermal stability 1517
5.3. Crystallization behavior 1518
5.4. Flame retardance 1518
5.5. Other properties 1519
5.5.1. Coefficient of thermal expansion 1519
5.5.2. Dielectric properties 1519
5.5.3. Wettability properties 1519
5.5.4. Self-healing properties 1519
6. Biomedical applications of HNTs-polymers nanocomposites 1519
6.1. Tissue engineering scaffold 1520
6.2. Drug/DNA carrier 1520
6.3. Cancer cell isolation 1521
6.4. Bone implants 1521
6.5. Cosmetic applications 1521
7. Conclusion and future prospects 1521
Acknowledgements 1522
References 1522

Nomenclature

AEAPS	[3-2-aminoethylamino) propyl]trimethoxysilane
AIBN	azo-bis-isobutryonitrile
APS	3-aminopropyltrimethoxysilane
APTES	(3-aminopropyl)triethoxysilane
ATRP	atom transfer radical polymerization
BBT	2,5-bis(2-benzoxazolyl) thiophene)
BDP	bis(diphenyl phosphate)
BNNTs	boron nitride nanotubes
C.O.F	coefficient of friction
CBS	N-cyclohexyl-2-benzothiazole sulfonamide
CNTs	carbon nanotubes
CTE	coefficient of thermal expansion
DCM	dichloromethane
DDS	drug delivery systems
DMF	dimethyl formamide
DPG	diphenyl guanidine
DRIFTS	diffuse reflectance infrared Fourier transform spectroscopy

EPB	2,2-(1,2-ethenediyldi-4,1-phenylene) bis-benzoxazole
EPD	electrophoretic deposition
EPDM	ethylene-propylene-diene monomer
FKM	fluoroelastomers
GPTS	γ-glycidoxypropyltrimethoxysilane
HA	hydroxyapatite
HNTs	halloysite nanotubes
HPC	hydroxypropyl cellulose
HRR	peak of heat release rate
LbL	layer-by-layer
LLDPE	linear low density polyethylene
MAPTS	3-(trimethoxysilyl)propyl methacrylate
MCA	melamine cyanurate
MDMA	magnesium dimethacrylate
MEL	melamine
MLR	peak mass loss rate
MMT	montmorillonite
MPS	methacryloxypropyltrimethoxy silane
NBR	butadiene-acrylonitrile rubber
NMR	nuclear magnetic resonance spectroscopy
NR	natural rubber
ODP	octadecylphosphonic acid
PA6	polyamide 6
PAA	polyacrylic acid
PAAm	polyacrylamide
PAH	poly(allylaminehydrochloride)
PAN	polyacrylonitrile
PANi	polyaniline
PBA	poly(butylenes adipate)
PBT	polybutylene terephthalate
PC	polycarbonate
PCL	poly(ε-caprolactone)
PEG	polyethylene glycol
PEI	polyetherimide
PES	polyethersulfone
PET	polyethylene terephthalate
PLA	polylactide
PLGA	poly(lactic-co-glycolic acid)
PMMA	poly(methyl methacrylate)
PMMA-b-PNIPAM	poly(methyl methacrylate)-b-poly(N-isopropylacrylamide)
PP	polypropylene
PP-g-MA	PP-graft-maleic anhydride
PPA	phenylphosphonic acid
PPy	polypyrrole
PS	polystyrene
PVA	polyvinyl alcohol
PVC	polyvinyl chloride
PVDF	poly(vinylidene fluoride)
SDS	sodium dodecyl sulfate
SEA	peak of specific extinction area
SEM	scanning electron microscope
TEM	transmission electron microscope
TGA	thermogravimetric analysis
VERs	vinyl-ester resins
VTMS	vinyltrimethoxysilane
XPS	X-ray photoelectron spectroscopy
XRD	X-ray diffraction
xSBR	carboxylated butadiene–styrene rubber
ZDMA	zinc dimethacrylate
ZDS	zinc disorbate

1. Introduction

Polymer nanocomposites containing organic and inorganic nanofillers have attracted extensive interest from academic and industrial perspectives due to the unique characteristics of nanoparticles, including their large surface area, high surface reactivity, and relatively low cost [1]. Traditional nanofillers include black carbon, graphite, silica, and silicate; these materials can enhance numerous polymer properties, generating increased mechanical properties, improved thermal resistance, and reduced gas permeability. The large aspect ratio, high strength, and relatively low density of 1D tube-like nanofillers have attracted intense research interest [2,3]. Numerous investigations have focused on carbon nanotubes (CNTs) and boron nitride nanotubes (BNNTs); both of these materials are technologically demanding to produce in bulk, making them expensive. Halloysite nanotubes (HNTs) offer an inexpensive, low-tech alternative that is morphologically similar to multiwalled CNTs. As a hydrated polymorph of the 1:1 phyllosilicate clay, specifically the kaolin group [4], HNTs are novel 1D natural nanomaterials with a unique combination of tubular nanostructure, large aspect ratio, natural availability, rich functionality, good biocompatibility, and high mechanical strength. These characteristics generate exceptional mechanical, thermal, and biological properties that are available at the low cost for HNTs-polymer nanocomposites [5,6]. HNTs also show potential during the controlled release of active agents. Therefore, HNTs may replace the more expensive CNTs in high-performance polymer nanocomposites and multifunctional nanocomposites.

The name ‘halloysite’ was first used in 1826 by Berthier [7] and was derived from Omalius d’Halloy, who found the mineral in Angleur, Liége, Belgium. The extensive research on halloysite began in the 1940s [8–12]. In recent years, halloysite has regained attention due in part to a surging interest in tube-like nanoparticles in materials science and technology. A survey of open publications related with halloysite to the past 20 years is shown in Fig. 1. These data were obtained based on a SciFinder Scholar search. The data clearly demonstrates that the halloysite has recently attracted more attentions, particularly in the last 6 years. A persistent growth in the number of publications is expected in the coming several years.

Raw halloysite is mined from natural deposits. This material is usually white in color but is also sometimes slight red (Fig. 2a). The stone-like raw halloysite is easily ground into powder (Fig. 2b). The molecular formula for HNTs is $Al_2Si_2O_5(OH)_4{\cdot}nH_2O$ (similar to kaolinite with water molecules) [13]. When $n=2$, the HNTs are in a hydrated state with one layer of water in the interlayer spaces. In this case, the materials are called HNTs-10 Å

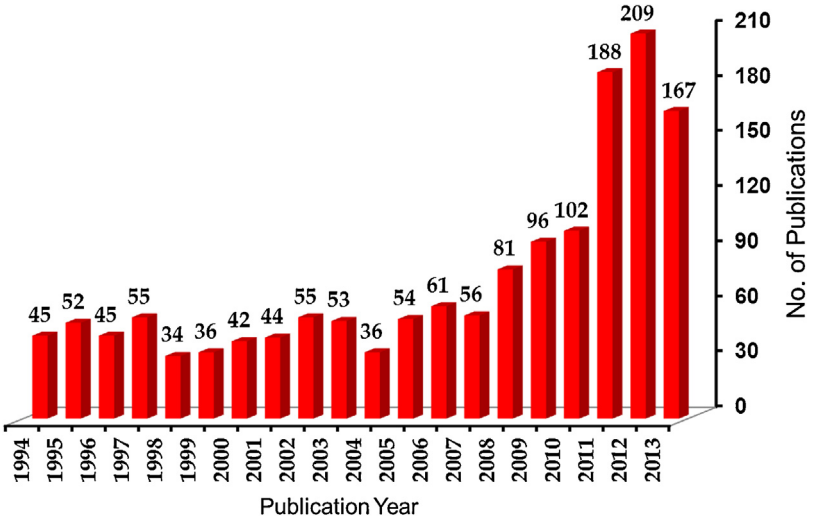

Fig. 1. Comparison of the annual number of scientific publications on the "halloysite" word in the past 20 years. (Data analysis of publications was done using the SciFinder Scholar search system with the term "halloysite", as at 4 September 2013).

[14]. When heating the HNTs-10 Å under mild conditions (30–110 °C), the water between the layers is lost, triggering an irreversible change into HNTs-7 Å. In this state $n = 0$. Morphologically, HNTs have a hollow tubular structure with a high aspect ratio (Fig. 2c and d), unlike kaolinite; kaolinite has a stacked-plate structure. Although spherical halloysite has also been found [15], we are not covering it in this article. Little information in the literature is available regarding the genesis of HNTs; however, some authors postulate that the tubular HNTs can be formed by rolling kaolin sheets in preference to tetrahedral rotation, correcting the fit of the octahedral and tetrahedral sheets in the soils of wet tropical and subtropical regions, as well as weathered rocks [16]. In addition, HNTs are multi-walled inorganic nanotubes. An ideal HNTs crystal consists of a layered structure that contains octahedrally coordinated Al^{3+} and tetrahedrally coordinated Si^{4+} in a 1:1 stoichiometric ratio (Fig. 2e) [4]. The HNTs range in length from 0.2 to 2 μm; the inner diameter and the outer diameter of the tubes range from 10 to 40 nm and 40 to 70 nm, respectively. In contrast to most clay, most of the aluminols are located in the interior of the HNTs, while the outer portions of the HNTs are primary siloxanes and few silanols/aluminols that are exposed in the edges of the sheets. The inner and outer surfaces of the HNTs are positively and negatively charged, respectively. The typical data for HNTs is shown in Table 1 [17]. HNTs have various applications as ceramic raw materials, nanocontainers for active compounds, catalysts, adsorbents, and polymer fillers.

In this article, we review the recent progress toward the development of HNTs-polymer nanocomposites, paying particular attention to the interfacial interactions of nanocomposite systems. The characteristics of HNTs related to the formation of polymer nanocomposites are summarized first. Covalent or non-covalent functionalization methods for HNTs and various fabrication approaches for the HNTs-polymer nanocomposites are subsequently introduced. The mechanical, thermal, biological, and drug sustained release properties of HNTs-polymer nanocomposites are described in detail. Finally, we provide an outlook for the future development of HNTs-polymer nanocomposites in various potential applications, including high-performance composites, tissue engineering scaffolds, wound dressing materials, drug delivery carrier, and cancer diagnosis materials.

2. Characteristics of HNTs relative to formation of polymer nanocomposites

2.1. Tubular microstructure

HNTs have tubular microstructures that ensure their high aspect ratio (typically ca. 10–50, see Table 1). The high aspect ratio of HNTs helps reinforce polymers in composites by optimising the load transfer from the matrix to the nanotubes. In addition, the elastic modulus of HNTs is 140 GPa (compared the theoretical value of 230–340 GPa) [18–20]. The mean particle size of HNTs in a 5 wt.% aqueous

Table 1
Typical analysis data of HNTs relative to formation of polymer nanocomposites.

Chemical formula	$Al_2Si_2O_5(OH)_4 \cdot nH_2O$
Length	0.2–2 μm
Outer diameter	40–70 nm
Inner diameter	10–40 nm
Aspect ratio (L/D)	10–50
Elastic modulus (theoretical value)	140 GPa (230–340 GPa)
Mean particle size in aqueous solution	143 nm
Particle size range in aqueous solution	50–400 nm
BET surface area	22.1–81.6 m^2/g [17]
Pore space	14–46.8%
Lumen space	11–39%
Density	2.14–2.59 g/cm^3
Average pore size	79.7–100.2 Å
Structural water release temperature	400–600 °C

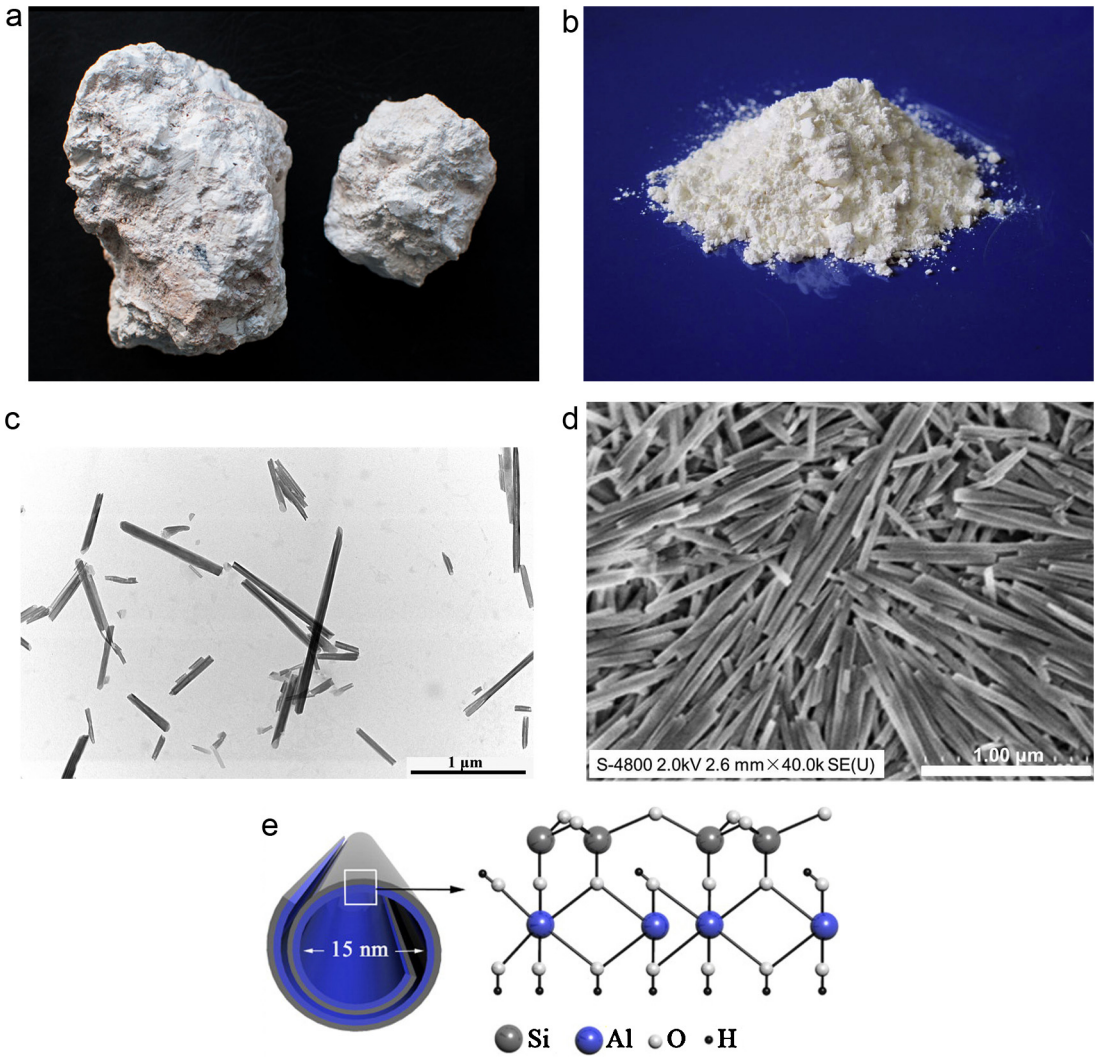

Fig. 2. The raw halloysite (a) and ground halloysite (b), TEM (c) and SEM (d) photos of HNTs minded from Hunan Province, China, and schematic illustration of crystalline structure of HNTs (e).
Source: [57] Copyright 2012. (d) and (e) are reproduced with permission from American Chemical Society, Washington DC, USA.

solution is 143 nm and their size ranges from 50 to 400 nm [21]. The high aspect ratio, small dimension, and high strength suggest that HNTs have a potential uses in high-performance polymer nanocomposites.

Compared to other nanoparticles, HNTs have a moderate BET surface areas value (22.10 m^2/g to 81.59 m^2/g) [17]. However, HNTs have a 10.7–39% lumen space. Due to the empty lumen structures, the density of HNTs is relatively low (2.14–2.59 g/cm^3) [22–24]; it is lower than other fillers, such as talc and calcite $CaCO_3$, and comparable to that of montmorillonite and kaolinite. The relatively low density of HNTs makes them convenient when preparing light-weight polymer composites.

HNTs have perfect tubular microstructures; therefore, many chemically and biologically active substances can be loaded into the lumen under vacuum or through immersion in the appropriate solution. Numerous drugs, such as tetracycline, khellin and nicotinamide adenine dinucleotide have been loaded into HNTs by soaking in a saturated drug solution under vacuum [25]. The drug released from the HNTs can last 30–100 times longer than the drug alone or in other carriers. Adding a polymer coating to the drug-loaded HNTs surface further slows the drug release rate. If the reactants are loaded into the tubes and reactions are induced, the tubes can act as nano-scale reactors. For example, Shchukin et al. employed HNTs as hollow enzymatic nanoreactors [26]. The urease-catalyzed deposition of $CaCO_3$ from an aqueous solution containing $CaCl_2$ and urea was undertaken inside the lumen of HNTs. The synthesized $CaCO_3$ completely filled the inner HNTs lumens; no $CaCO_3$ formed on the outer surface of the HNTs or in solution. The lumen of the HNTs also can entrap the polymer

chains or decomposition products, delaying the degradation of the polymer and increasing its thermal stability and flame retardance.

2.2. Relatively "hydrophobic"

Most of the aluminols locate inside the HNTs, while in the outer surface of the HNTs are primarily siloxane with a few silanols/aluminols exposed on the edges of the sheets. Compared to other nanoclays and nanosilica, the relatively low content of hydroxyl groups on their surfaces makes HNTs relatively hydrophobic. Therefore, HNTs can be readily dispersed in non-polar polymers using shear due to the interactions between the tubes and the polymer backbone [27–30]. The natural hydrophobicity of HNTs is not sufficient for interfacial adhesion in composite systems. Further hydrophobic treatment of HNTs should be performed before adding them into polymers to maximize their interfacial interactions.

2.3. Relatively low tube-tube interactions

In general, nanoparticles tend to attach to one other due to their high surface activities. For example, CNTs have a strong intrinsic van der Waals attraction between nanotubes, making dispersion in common solutions and polymers challenging [31]. In contrast, HNTs have relatively few tube–tube interactions due to the following two aspects. Chemically, few hydroxyl groups and siloxane are located on the HNTs surfaces, revealing that the tube–tube interactions are relatively weak. Geometrically, the tube-like morphologies with a proper aspect ratio generate few opportunities for large-area contact between tubes. Consequently, a uniformly dispersed morphology is usually obtained in HNTs-polymer nanocomposites [5]. This naturally exfoliated morphology means that the particles no need to be chemically separated, benefiting the industrialization of the HNTs-polymer nanocomposites.

2.4. Reinforcing

Due to the high aspect ratio of HNTs and their nanoscale dimensions, HNTs are excellent reinforcement materials for different polymers. More importantly, the interfacial interactions between the HNTs and the polymers can be tailored using chemical or physical approaches. Almost every polymer can be mechanically reinforced by HNTs, even at low loadings (5 wt.%). The strength, modulus, stiffness and impact resistance of polymers can be increased simultaneously by HNTs. Additionally, HNTs can enhance the mechanical properties of the polymers at high temperatures under both dynamic or static conditions. For instance, the coefficient of thermal expansion (CTE) for epoxy resin significantly decreased after incorporating HNTs [21], because the expansion of the polymer matrix was constrained by the presence of inorganic filler.

2.5. Flame retardance

HNTs can be used as halogen free flame retardants in polymers due to the barriers against heat and mass transport when burning the nanocomposites, as well as the entrapment of polymer decomposition products in the lumen. In addition, the presence of iron in the HNTs decreases the flammability of the composite [32]. An additional flame retardance mechanism attributed to HNTs in some polymers, such as polycarbonate (PC) and PC/ABS blend, has been correlated to the promotion of char formation due to their surface acidity [33,34]. HNTs have a high structural water release temperature (400–600 °C) [4], meaning that HNTs are suitable for polymers processed at relatively high temperatures. HNTs can be employed as a flame retardant in polypropylene (PP), liner low density polyethylene (LLDPE), polyamide 6 (PA6), polybutylene terephthalate (PBT) and polyethylene terephthalate (PET).

2.6. Hydroxyl groups distribution

HNTs with aluminum on the innermost surfaces and silicate on the outermost surfaces facilitate different inner/outer surface chemistry. Therefore, selective modification of the silica or alumina in HNTs can be realized through successive reactions with phosphonic acid (interior) and silylating (exterior) agents. Bifunctionalizing HNTs produce a new type of adsorbent with tunable properties. For example, the hydrophobic lumen can encapsulate neutral and hydrophobic guest molecules by partitioning with a polar solvent, while the solid polar shell stabilizes the dispersion of the nanotube in water and retains the guest molecules [35].

2.7. Negatively charged surfaces

The surface charge of HNTs is predominantly negative over most of the physiologically relevant pH range (>2), facilitating electrostatic attractions with cationic polymers. These interactions can be used when designing the interface of polymer nanocomposites. For example, the layer-by-layer (LbL) assembly of HNTs and polyetherimide (PEI) can used to preparing HNTs-PEI nanocomposites [36]. The positively charged chitosan can interact electrostatically with the HNTs, which is employed for the composites preparation [37].

2.8. Electrophilic

HNTs are electrophilic. The electron acceptor sites on HNTs are the aluminum species at the crystal edges and the transition metals in the higher valences of the silicate layers. HNTs can accept electrons from the vinyl monomer, helping to catalyze the polymerization of some unsaturated organic compounds (styrene, hydroxyethyl methacrylate) [38]. The electrophilic properties of HNTs can also be used to enhance the interfacial interactions in the polymer nanocomposites [39].

2.9. Porosity and the surface defects

HNTs have a regular tubular morphology, bulk structure and rich mesopores (14–46.8% pore space). The pore size distribution for HNTs is broadly bimodal. The peak 1 is attributed to internal/surface pores, including spaces

between the overlaps of folded HNTs sheets, and peak 2 is attributed to the central lumen of the tubes [17]. If the nanospace in HNTs is filled or its surface is coated with polymers, the porous materials that are extracted from the HNTs framework will reflect the morphology and pore structure of the HNTs template. For example, HNTs can be used as a template for mesoporous carbon. There are two main advantages for HNTs templates [40]: (1) the diameter of the tube is on nanometer scale, promoting the penetration of the carbon source into the HNTs matrix; (2) HNTs area natural mineral, reducing the cost of templated mesoporous carbon.

2.10. Abundant deposition, easily available and cheap

HNTs are "green" materials: they are not hazardous toward the environment. Thousands of tons of HNTs are available from natural deposits in countries such as China, America, Brazil, France, Spain, New Zealand and others [41–43]. For many applications, microcylinders made from carbon or lipid nanotubes are cost prohibitive. HNTs are a viable alternative for applications in which cost sensitivity is an issue. The low price and high performance facilitate the industrialization of HNTs-polymer nanocomposites.

3. Functionalization of HNTs for polymer nanocomposite preparation

As discussed above, HNTs have numerous advantages benefiting polymer nanocomposite formation. However, to optimize the properties of the desired composites, the nanotube dispersion and stress transfer must be optimized. Additionally, the interface between the nanotube and the polymer must be carefully engineered; otherwise, poor load transfer between the nanotubes and surrounding polymer chains may cause interfacial slippage, decreasing the mechanical properties of the composites. Therefore, functionalizing HNTs is extremely important for processing and enhancing the properties of HNTs-polymer nanocomposites. The polymer nanocomposites based on modified nanotubes exhibit improved mechanical and thermal properties, because the functionalization improves the dispersion and stress–strain transfer. In this section, the purification of raw halloysite is introduced. Afterward, two major functionalization approaches for HNTs (covalent functionalization and non-covalent modifications) are introduced. For drug delivery systems (DDS) and nanomaterial storage applications, opening and blocking pores is critical. Therefore, methods for opening and blocking the pores in HNTs are described.

3.1. Purification of HNTs

Raw halloysite is mined directly from nature; therefore, the impurities, such as quartz, kaolinite, illite, feldspar, perlite, and metal ions, should be removed and the aggregates tubes should be separated before use. The purification methods for HNTs are based on a dispersion–centrifugation–drying technique [26,39,44]. The most common routine is provided below. A 10 wt.% water suspension is prepared by slowly adding halloysite powder to deionized water with stirring. The dispersion of the halloysite particles is increased by heating to 60 °C for 12 h while with stirring. The resulting product is separated using centrifugation and washed three times with distilled water. Finally, the purified HNTs are dried at 60 °C in air for 12 h, generating the dehydrated HNTs-7 Å form. Before use, the dry HNTs are sieved to eliminate any aggregates formed during drying. To increase the stability of halloysite in water and facilitate individualization, such as sodium hexametaphosphate [39] and Tween 80 [44], can be added into the suspension. Interestingly, nearly pure halloysite deposits have been found in Utah, USA [45,46], that do not require purification before use.

3.2. Covalent functionalization

The hydroxyl groups located on the inner surfaces and in the edges of the sheets forming the multi-walled tubes provide reactive sites for covalently attaching chemical species. After choosing an appropriate method, the following effects are expected [47]:

- The polarity of the HNTs surface can be reduced.
- The hydroxyl groups on the surface can be shielded.
- The chemical composition of the surface can be changed to include hydrocarbons.
- Functional groups can be created on the surface.

Covalent functionalization can improve the dispersion of the HNTs in solvents and polymers by increasing their interfacial compatibility. The increased interfacial adhesion further optimizes the nanocomposite properties by facilitating the stress or heat transfer through the interfaces.

3.2.1. Silane coupling

The most common covalent modification to HNTs is grafting silanes via condensation between the hydrolyzed silanes and the surface hydroxyl groups of the HNTs [48]. The aluminol groups are located on the internal surface of the lumen, while the aluminol and silanol groups are located on the edges or on external surface defects. Modifying the internal surface is relevant for immobilization and controlled release applications, while modifying the external surface and edges benefits for nanocomposite applications. Although the siloxane surface of HNTs is generally regarded as nonreactive, some results indicate that the hydroxyl groups at defect sites are available for modification. The grafting reactions can occur in either toluene or water/alcohol mixtures. Various silanes have been grafted onto HNTs when preparing polymer composites (Table 2).

Yuan et al. modified HNTs by grating organosilane APTES and suggested a reaction mechanism [48]. They found that the modification included not only the direct grafting of APTES onto the surface hydroxyl groups, but also oligomerization; the hydrolyzed APTES condensed with itself and the already grafted APTES to form a cross-linked structure (Fig. 3). An evacuation pretreatment can dramatically enhance the loading of hydrolyzed APTES into the lumen of HNTs and increase the grating ratio.

Table 2
The chemical composition of silanes used for modification of HNTs.

Name	Chemical composition
γ-Glycidoxypropyltrimethoxysilane (GPTS) [49]	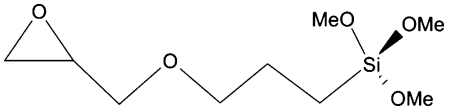
3-Aminopropyltrimethoxysilane (APS) [55,56]	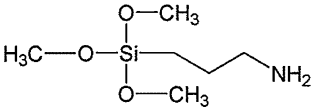
(3-Aminopropyl)triethoxysilane (APTES) [48,132]	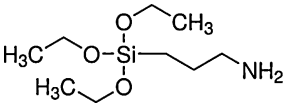
[3-(2-Aminoethylamino)propyl]trimethoxysilane (AEAPS) [35,145,146]	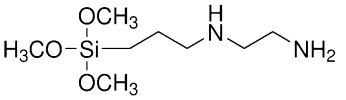
3-(Trimethoxysilyl)propyl methacrylate (MAPTS) [50,53]	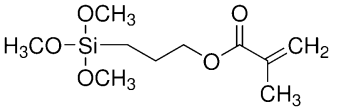
Vinyltrimethoxysilane (VTMS) [88]	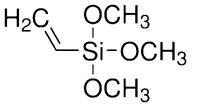

Coupling agents including GPTS and MAPTS were grafted on HNTs to increase the interfacial adhesion of the HNTs-polymer nanocomposites [49]. The grafting reaction was performed in an ethanol/water mixture, and the grafted product was analyzed by thermogravimetric analysis (TGA), pore analysis based on nitrogen adsorption–desorption, X-ray photoelectron spectroscopy (XPS) and nuclear magnetic resonance spectroscopy (NMR). The graft ratio was 2.4–4.9 wt.% (relative to HNTs) by TGA. The pore analysis and XPS also confirmed the grafting of silanes on HNTs. When the grafted weight of the silane was low, its verification through the comparison of

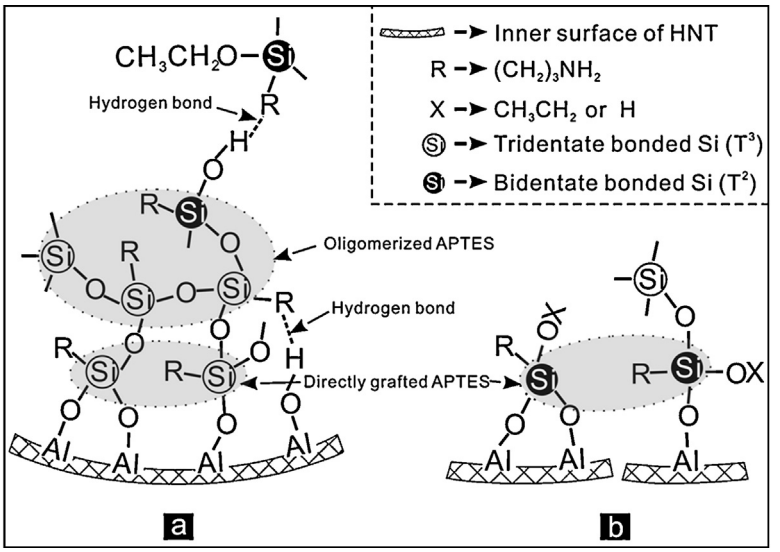

Fig. 3. Schematic representation of the mechanism of the formation of cross-linked network of APTES (a), and of the grafting between bidentate bonded Si and AlOH groups on HNTs (b).
Source: [48] Copyright 2008. Reproduced with permission from American Chemical Society, Washington DC, USA.

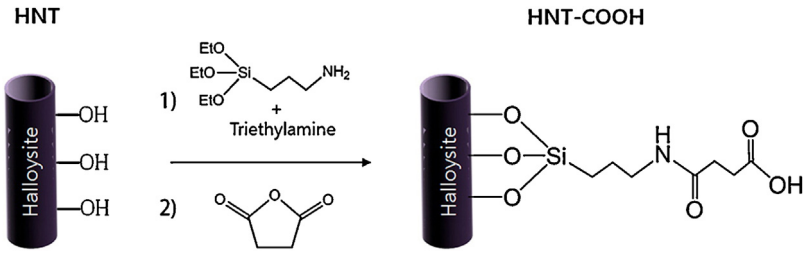

Fig. 4. Modification of pure HNTs to carboxylic acid functionalized HNTs-COOH.
Source: [51] Copyright 2012. Reproduced with permission from American Chemical Society, Washington DC, USA.

FTIR spectra was hard. However, when the graft weight was relatively high or when using diffuse reflectance infrared Fourier transform spectroscopy (DRIFTS), the grafted silanes on HNTs could be identified [48,50].

Apart from being used directly in HNTs-polymer nanocomposites, the silane grating methods can also be employed as a pretreatment before additional surface modifications. For example, to prepare HNTs-COOH, HNTs were first modified with amino groups by grating APTES. Afterward, the HNTs-NH_2 product was mixed and stirred with succinic anhydride in dimethyl formamide, generating the HNTs-COOH (Fig. 4) [51].

3.2.2. Surface graft polymerization

Several polymers can be grafted onto HNTs using different polymerization mechanisms. For example, grafting of poly(butylenes adipate) (PBA) chains from the hydroxyl-groups on the HNTs surface was performed in two steps [52]. During the first step, the hydroxyl groups on the HNTs surfaces were reacted with dimethyl adipate in a condensation reaction. Afterwards, additional dimethyl adipate was added with 1,4-butanediol to grow poly- or oligoester chains at the HNTs surfaces (Fig. 5). TGA analysis indicated that the amount of PBA grafted on the HNTs surface was about 3 wt.%. The PBA-grafted HNTs can improve the interfacial adhesion between HNTs and the polyvinylchloride (PVC) matrix. Poly(methyl methacrylate) (PMMA) was grafted onto HNTs via in situ free radical polymerization [53,54]. The surface of the HNTs was first functionalized with MAPTS. Afterward, MMA (monomer), isopropanol (solvent), and azo-bis-isobutryonitrile (AIBN) (initiator) were mixed and reacted with MPS-HNTs. The percentages of grafting and grafting efficiency of MMA to HNTs were 11.4% and 17.8%, respectively. The PMMA-grafted HNTs had a increased water contact angle, indicating that their polarity was reduced. The PMMA-g-HNTs could surpass the basic mechanical performance of epoxy acrylate composites, particularly regarding toughness and wear resistance.

Atom transfer radical polymerization (ATRP) can also be employed to modify the surface of HNTs or to prepare HNTs-polymer nanocomposites directly [55–57]. For example, polystyrene (PS) and polyacrylonitrile (PAN) were grafted onto HNTs, generating composite nanotubes. The HNTs were first modified with APS, subsequently immobilizing an ATRP initiator (2-bromoisobutyrylbromide). Afterward, an ATRP with styrene or acrylonitrile was carried out simultaneously on the interior and exterior surfaces of the HNTs. The polymer-modified HNTs

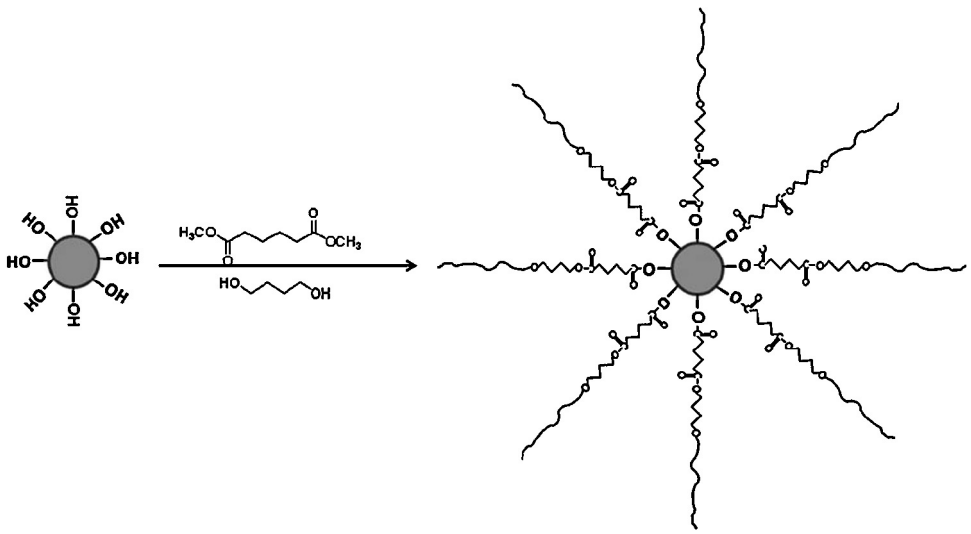

Fig. 5. Synthesis of the PBA grafted HNTs.
Source: [52] Copyright 2011. Reproduced with permission from Royal Society of Chemistry, UK.

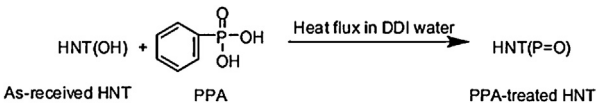

Fig. 6. Modification of HNTs by phenylphosphonic acid (PPA). *Source:* [60] Copyright 2011. Reproduced with permission from Elsevier Science Ltd., Oxford, UK.

could convert into carbon-HNTs via carbonization. Finally, free-carbon nanotubes or nanowires were formed by dissolving the HNTs with a hydrofluoric acid/hydrochloric acid mixture. Another HNTs-polymer nanocomposite was prepared through an in situ oxidative polymerization of pyrrole [58]. The prepared HNTs-polypyrrole (PPy) hybrids were pyrolyzed to form a HNTs-carbon hybrid. Lastly, mesoporous carbon was obtained after removing the HNTs with acid. Similarly, PMMA can be grafted onto HNTs by immobilizing an ATRP initiator and proceeding with the polymerization reaction [57].

Plasma polymerization uses plasma sources to generate a gas discharge that provides the energy needed to activate or fragment gaseous or liquid monomers that often contain a vinyl group, initiating polymerization. This technique can be used to modify the properties of HNTs surfaces. Poikelispää et al. used pyrrole and thiophene as monomers for plasma polymerization on HNTs [47]. The pyrrole- and thiophene-coated HNTs were more hydrophobic and less polar than the untreated HNTs. The plasma-treated HNTs exhibited good dispersion while reinforcing a natural rubber (NR)–butadiene rubber blend.

3.2.3. Covalently grafting phosphonic acid

Phenylphosphonic acid (PPA) can be used to unfold and intercalate HNTs [59,60]. The dehydrolysis reaction occurred between the hydroxyl groups on the HNTs and the phosphonic acid groups of the PPA (Fig. 6). The PPA treatment increased the basal spacing from 7.2 Å to 15.1 Å, changing the morphology of most of the particles from nanotubes to nano-platelets. Better dispersion and higher mechanical performance in the epoxy were achieved by using the PPA-treated HNTs compared to the as-received HNTs.

The inner lumen of the HNTs can be modified with octadecylphosphonic acid (ODP) [35]. The typical procedure is shown below. The HNTs were mixed with ODP in EtOH:H_2O. Afterward, the suspension was transferred into a vacuum jar that was then evacuated several times. The bubbling observed in the suspension indicated that air was removed from the lumen of the tubules and replaced with the ODP solution. After stirring for a week at room temperature, the modified HNTs were rinsed, centrifuged, and dried. The ODP bonded to the alumina sites at the tube lumen but not the outer siloxane surface. Therefore, the ODP-modified HNTs can be modified further by coupling silane AEAPS on their outer surfaces (Fig. 7). This selective modification created an inorganic micelle-like architecture with a hydrophobic aliphatic chain core and a hydrophilic silicate shell. These modified HNTs could be used for water purification, as well as drug immobilization and controlled release. For example, ODP-modified HNTs were loaded with hydrophobic bisphenol-A bis(diphenyl phosphate) (BDP) (flame retardant for polymers). The

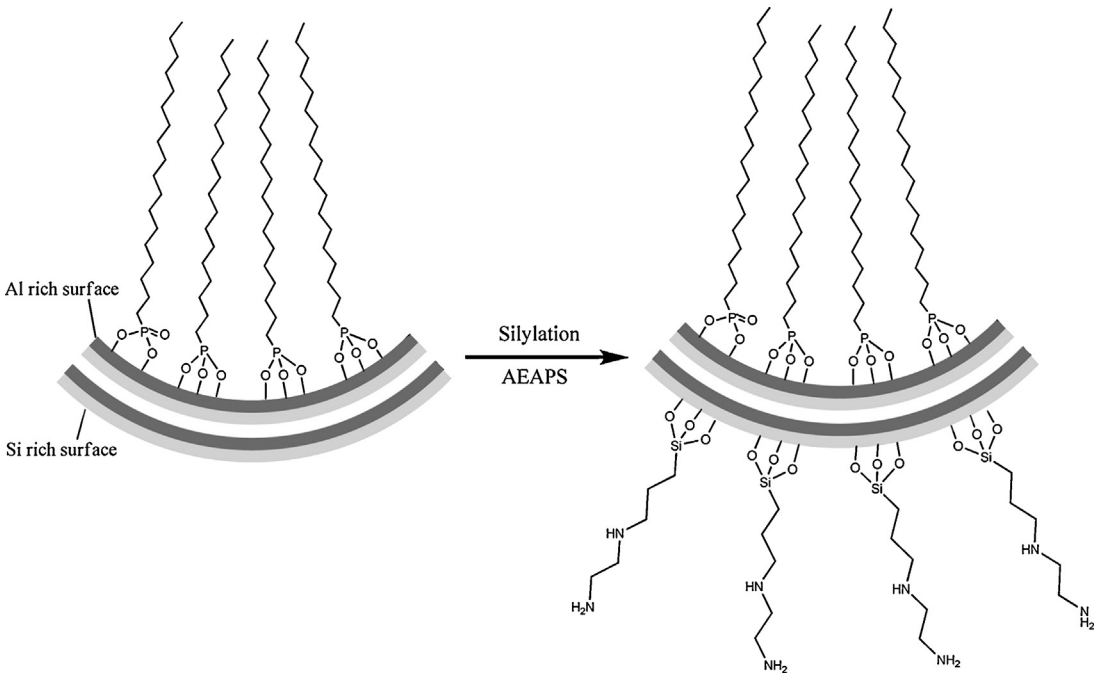

Fig. 7. Schematic illustration of bifunctionalization of the silica–alumina oxide surface of HNTs by ODP and subsequent AEAPS silylation. *Source:* [35] Copyright 2012. Reproduced with permission from American Chemical Society, Washington DC, USA.

modified HNTs had a high BDP loading ability. Additionally, this flame retardant was released from the nanotubes in linear fashion over 60 h, demonstrating their potential utility as effective nanocontainers for smart composite systems [61].

3.3. Non-covalent functionalization

3.3.1. Non-covalent functionalization based on electron transfer interactions

The relatively low hydroxyl group content on the surface of the HNTs limits the reactive sites for covalent bonding. Consequently, modifying HNTs using covalent linking methods is usually unsatisfactory. Fortunately, the presence of several metallic atoms on HNTs, such as aluminum, iron and transition metals with unoccupied orbitals, offers numerous opportunities for improving the interfacial properties of HNTs and polymers or organic molecules via electron transfer interactions [38,62]. 2,5-bis(2-benzoxazolyl) thiophene (BBT) [39] and 2,2-(1,2-ethene diyldi-4,1-phenylene) bisbenzoxazole (EPB) [63] are capable of donating electrons. These compounds were mechanically mixed with HNTs, and the mixtures were added to PP to confirm the modification. BBT and EPB positively affected the HNTs-imparted reinforcement of PP. For example, BBT was aligned to form a fibril structure with HNTs when processing the nanocomposites due to electron transfer interactions. The formation of the BBT fibrils imparted higher crystallinity compared to the PP-unmodified HNTs nanocomposites. The nanocomposites with BBT also showed substantially increased mechanical properties. This approach improves the interfacial properties in situ.

3.3.2. Non-covalent functionalization based on hydrogen bonding interactions

Several organic species including melamine (MEL), melamine cyanurate (MCA) and diphenylguanidine (DPG) can interact with HNTs via hydrogen bonding [64,65]. This behavior can be utilized to construct a filler network in polymers via self-assembly. The organic molecules and HNTs were added simultaneously to the polymers during processing. With this methodology, the flexural modulus of the PP nanocomposites was improved up to 80% due to an optimal combination of HNTs and organic hydrogen-bonding couplers. This hydrogen-bonding-induced assembled filler network also reinforced polar PA6; this process could be used with other inorganic materials, such as nanosilica. Functionalizing HNTs in this manner provides a general method for reinforcing polymers that has many advantages such as “green processing”, unsophistication, facile scale-up, cost effectiveness, etc.

3.3.3. Non-covalent functionalization based on electrostatic attraction interactions

As discussed above, HNTs can interact with cationic polymers, such as chitosan and PEI via electrostatic attraction. Apart from being used to prepare HNTs-cation polymer nanocomposites, these interactions can also be employed for the surface-treatment of HNTs. Coating HNTs with cationic polymers that bind onto the negative charges present on the tubule surface (charge neutralization) can slow down drug release [66,67].

3.3.4. Intercalation of HNTs

HNTs can be intercalated with salts and organic compounds; this behavior has been thoroughly reviewed by Joussein et al. [4]. However, in contrast to montmorillonite (MMT), HNTs did not need to be intercalated before adding them to polymers because HNTs have a tubular microstructure and good dispersion. Therefore, few works have focused on improving the effects of HNTs on polymers using intercalation [68]. The intercalation of urea into the HNTs was performed mechano-chemically (dry grinding). The urea-intercalated HNTs reinforce PP better than unmodified HNTs.

3.4. Enlargement of the lumen in HNTs or opening the inner-pores

Many applications for HNTs are constrained by the size of the lumen; therefore, enlarging the lumen using a chemical treatment is important. Due to the different internal/external chemistry, the selective etching of alumina from the inside of the tube was realized in a reaction with 0.5–2 M sulfuric acid; this process preserved the external HNTs diameter (Fig. 8) [69]. The lumen diameter changed from 15 to 25 nm, increasing the tube lumen capacity by 2–3 times for the loading and sustained release of active chemical agents. In particular, the HNTs loading efficiency for benzotriazole increased 4-fold by selectively etching 60% of the alumina. The specific surface area of the tubes increased more than 6-fold (40–250 m^2/g) upon acid treatment.

In another report, White et al. investigated the stability of HNTs in acidic and alkaline aqueous suspensions [70]. They found that progressively thinning the tubes from the inside could be initiated by the dissolution of the inner Al–OH catalyzed by acidic or basic species. In strong acidic solutions (1 mol dm^{-3} H_2SO_4), the greater solubility of Al(III) versus Si(IV) formed small SiO_2 nanoparticles inside the tubes, enhancing the surface area and pore volume of the sample. In 1 mol dm^{-3} NaOH solutions, the greater solubility of Si(IV) versus Al(III) formed fragmented flaky particles containing layers of $Al(OH)_3$. The acidic and alkaline treatment methods provided a convenient tool for increasing the specific surface area and pore volume of the HNTs without significantly altering of their shape. In particular, the ability to make the walls of the HNTs thinner in concentrated NaOH solution without creating SiO_2 nanoparticles inside the tubes may prove useful in applications where a larger internal diameter is required, such as the encapsulation of large protein or DNA molecules.

The inner diameter of HNTs is approximately 15–100 nm; therefore, they are a mesoporous material. Joo et al. found that the porosity could be tailored by changing the pH of a water suspension containing HNTs [71]. HNTs can act as doors for one another, blocking the inner-pore through aggregation or opening it through dispersion (Fig. 9). The inner-pores of HNTs were open after basic treatment through negative charge dispersion;

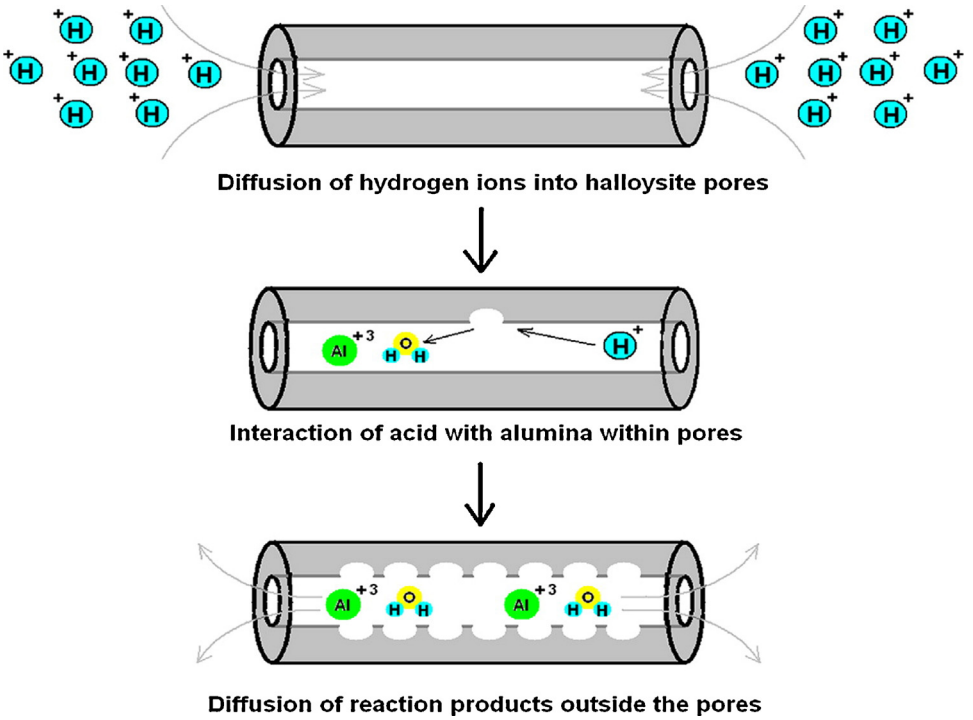

Fig. 8. Enhancement of the lumen by acid etching of alumina in inner layers of HNTs.
Source: [69] Copyright 2012. Reproduced with permission from American Chemical Society, Washington DC, USA.

they were closed after acidic and neutral treatments. The characteristics of HNTs pores could be applicable for drug delivery systems and the nano-material storage.

4. Main strategies for the fabrication of HNTs-polymer nanocomposites

4.1. Processability

The processablity of nanofiller is critical for its practical applications. Compared to CNTs-polymer nanocomposites, the HNTs-polymer nanocomposites exhibit better processability. First, the tube-tube interactions of HNTs are relatively weak, facilitating good dispersion by shear during processing. The surface-pretreatment for HNTs is not a necessary when forming polymer nanocomposites. HNTs have hydrophilic groups and small dimensions, enabling their dispersion in water via mechanical stirring or ultrasonic treatment. Consequently, they can be directly mixed with water-soluble polymers in aqueous solutions when preparing nanocomposites. Second, the melt or solution viscosity of polymers is only moderately influenced, even at high HNTs loading. For example, rheological investigations showed that the shear viscosity was only moderately increased after adding a small amount of HNTs to PA6, and nanocomposites with 30 wt.% HNTs could be still processed under similar conditions as neat PA6 [23]. Another example was that the maximum loading of HNTs in a polyacrylamide (PAAm)-HNTs nanocomposite hydrogel could 30 wt.%, while the maximum loading of Laponite in PAAm hydrogel was only 10 wt.% [72]. Third, HNTs can act as nucleating agents for different polymers; adding HNTs can modify the process ability of a crystallized polymer by shortening the processing time and enhancing the properties of the product. For example, the crystallization rate of polylactide (PLA) is rather slow, leading to a lengthy processing period and poor heat resistance. Adding a small amount HNTs to PLA can increase the crystallization rate, shorten the processing time and improve the heat resistance of the nanocomposites [73].

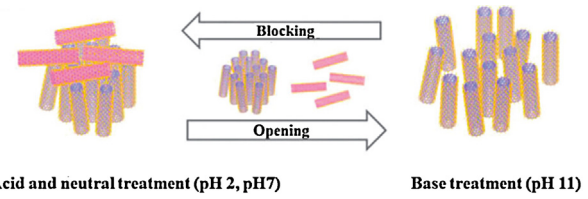

Fig. 9. Schematic illustration of the inner-space of HNTs after treatment with different pH solutions. The inner-spaces of HNTs were exposed through removal of obstructing HNTs. Purple: Al (bundle tube), pink: Al (cover tube), red: O, white: H, and yellow: Si.
Source: [71] Copyright 2013. Reproduced with permission from Royal Society of Chemistry, UK.

HNTs have a promising flow in polymer melts or polymer solutions under shear force during processing due to their proper aspect ratio and comparable density with the polymer. The flow of HNTs orients the tubes in the polymer matrix, enhancing the polymer performance. Fig. 10 shows the orientation of the HNTs in a PP melt with an interfacial modifier. Fig. 11 shows the orientation state of the HNTs in PLA matrix during a simple injection molding procedure.

The wide-angle X-ray diffraction (XRD) can quantify the degree of HNTs alignment in nanocomposites. The

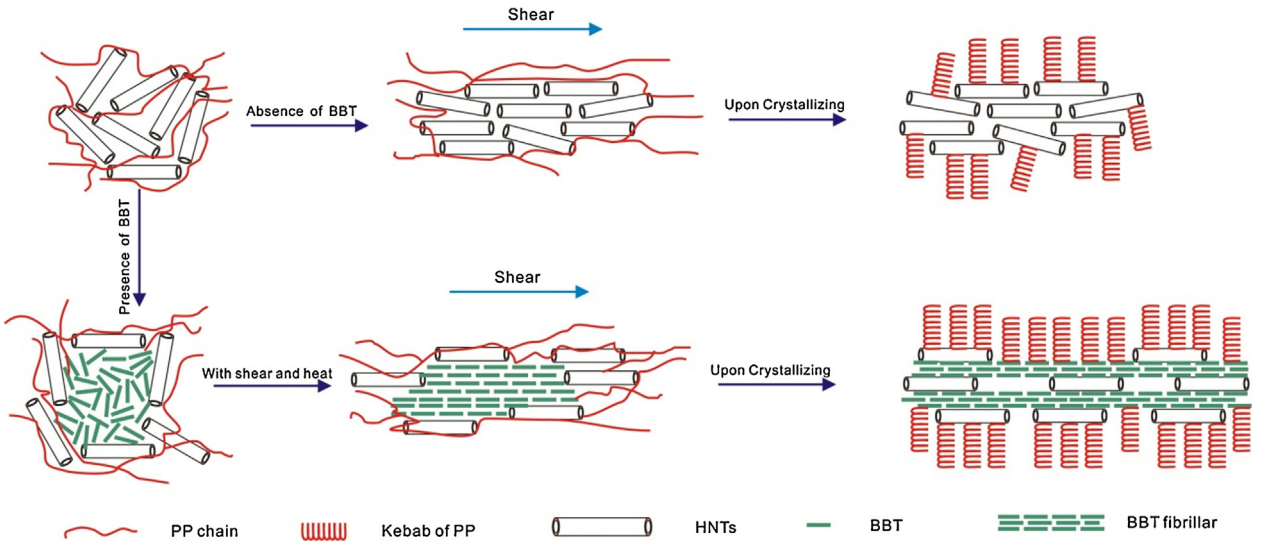

Fig. 10. Schematic of the orientation and the crystallization structure formation of HNTs-PP nanocomposites with or without an interfacial modifier BBT. *Source:* [39] Copyright 2008. Reproduced with permission from IOP Publishing, UK.

nanotube orientation may affect the properties of the composite. In XRD patterns, HNTs exhibit a basal peak at ~7 Å (0 0 1 reflection related to layer spacing) and a peak in the range of 4.41–4.46 Å (related to the disordered 0 2 0 and 1 1 0 reflection) [9]. When HNTs have a uniform of orientation in a polymer matrix, the intensity of 0 2 0 reflection may decrease or disappear. For example, in a HNTs-PLA nanocomposite and HNTs-PAAm nanocomposites, the reflection of HNTs at approximately 20° decreased or disappeared in the polymer nanocomposites even at low HNTs loading (5 phr) due to preferential orientation of the nanotubes in the polymer matrix [72,73]. This orientation was similar to oriented tiles patterns and was induced via shear force during processing. The orientation of the nanotubes suggested interfacial interactions occurred between the PLA chain and the HNTs. The alignment of the HNTs was confirmed by their scanning electron microscope (SEM) and transmission electron microscope (TEM) images. The orientation of the HNTs improved the mechanical and thermal properties of the polymer nanocomposites, since it led to 2D homogenization of the nano fillers in polymer matrix. A similar change in the XRD pattern of the HNTs in a polymer matrix was also found in HNTs-NR nanocomposites [74].

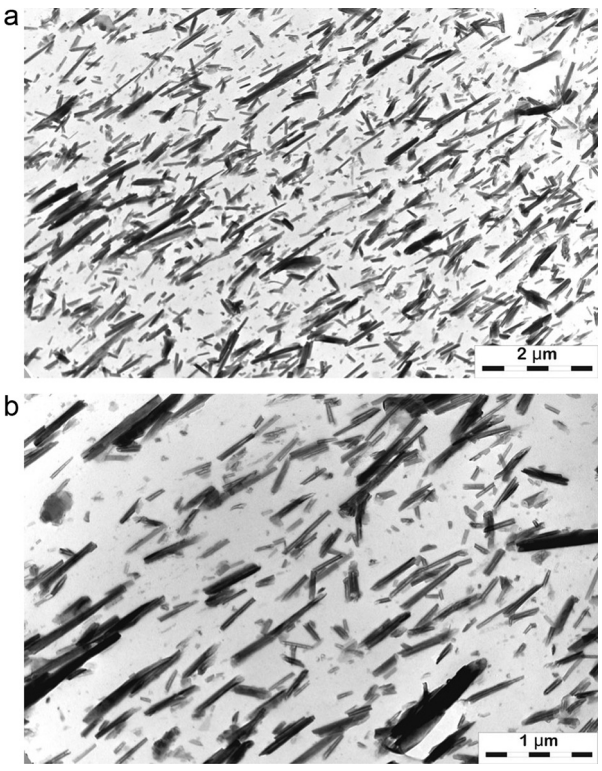

Fig. 11. TEM photos of HNTs-PLA nanocomposites with 30 phr HNTs, showing the orientation of the HNTs in the matrix (unpublished work).

4.2. Approaches for fabricating HNTs-polymer nanocomposites

HNTs can be mixed with almost all the plastics and rubbers using traditional methods with instruments such as the twin screw extruder and the two roll mill. The selection of fabrication methods has mainly focused on improving nanotube dispersion and enhancing interfacial interactions. In this section, we introduce the common processing methods used for HNTs-polymer nanocomposites.

4.2.1. Solution processing

Solution mixing is the most commonly method used for fabricating HNTs-polymer nanocomposites, because it is easily performed and suitable for small sample sizes. This process is realized by first dispersing the nanotubes and polymer in a suitable solvent (including water and organic solvent) with rigorous stirring or ultrasonic treatment, respectively. Finally, the HNTs-polymer nanocomposites

as film or hydrogels are obtained after precipitation or casting. Freezing the HNTs-polymer mixture in an aqueous suspension and reducing the surrounding pressure allows the frozen water to sublimate directly, leaving porous HNTs-polymer nanocomposite scaffolds. The relatively weak tube–tube interactions and other structural features make HNTs readily dispersible in polar solvents via stirring. To improve their dispersion and increase interfacial interactions, ultrasonication can be used to make metastable suspensions of HNTs or HNTs/polymer mixtures indifferent solvents. The dispersion of HNTs in solvent can be visually observed or determined via laser particle analysis. However, well-dispersed HNTs can re-aggregate in the polymer matrix during drying. This behavior should be considered when understanding the properties of the nanocomposites [75].

Polyvinyl alcohol [44,75–77], chitosan [37,78], pectins [79], hydroxypropyl cellulose [80], polyethylene glycol (PEG) [81], potato starch [82], poly(vinylidene fluoride) (PVDF) [83], containing PVC [52] can be mixed with HNTs in solution and cast to form nanocomposite films. HNTs-alginate nanocomposite gel beads can be prepared by mixing the HNTs in water and crosslinking them using calcium ions [84]. Latex rubber can also be mixed with HNTs, and a co-coagulation process can be utilized to prepare HNTs-rubber nanocomposites [85]. These nanocomposites exhibit significantly enhanced properties, especially mechanical ones.

4.2.2. Melt processing

Solution processing techniques cannot be utilized for insoluble polymers and are inefficient because they involve the removal of solvent. In these cases, melt processing is an alternative that is particularly useful for dealing with thermoplastic and rubber. Furthermore, melt processing is always simple and easy to integrate into standard industrial facilities, making it a most promising approach for producing HNTs-polymer nanocomposites industrially. The disadvantage of melt processing is the unexpected polymer degradation and oxidation that occur at high temperatures, as well as the strong shear force, leading to the decreased polymer properties. Generally, melt processing involves mixing HNTs with a molten polymer via shear force in different instruments. Afterward, HNTs-polymer nanocomposites can be prepared via compression molding, injection molding, or extrusion. Almost all the thermoplastics, rubbers and biopolymers have been mixed with HNTs using the melt processing approach (Table 3). When processing a HNTs-polymer nanocomposite, the polymer chains can interact with the HNTs due to the strong shear force, leading to interfacial compatibility. The surface-treatment of HNTs can improve the interfacial interactions with polymers during melt processing [39,50].

4.2.3. In situ polymerization

As discussed above, dispersing nanotubes in a liquid (monomer, solvent) followed by polymerization is employed to treat the surfaces of the HNTs or to prepare HNTs-polymer nanocomposites. Compared to solution mixing, in situ polymerization can improve the initial dispersion of the nanotubes in the monomer and, therefore, in the nanocomposites. More importantly, in situ polymerization techniques generate covalent bonds between the HNTs and the polymer matrix, generating hybrid materials.

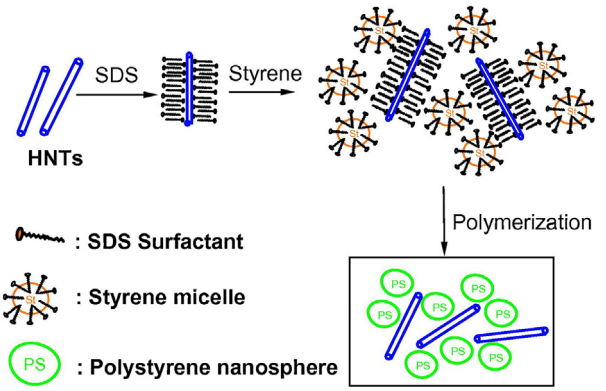

Fig. 12. A schematic picture showing the in situ polymerization of styrene in the presence of HNTs.
Source: [90] Copyright 2011. Reproduced with permission from Elsevier Science Ltd., Oxford, UK.

HNTs were dispersed in the epoxy resin [21,86,87], unsaturated polyester [88], and vinyl-ester resins (VERs) [24] before the resin was cured, forming organic–inorganic hybrids. Poly(methylmethacrylate)-b-poly(N-isopropylacrylamide) (PMMA-b-PNIPAM) nanocomposites and HNTs were synthesized via reverse ATRP [89]. High-impact PS nanocomposites filled with individually dispersed HNTs were also prepared via the emulsion polymerization of styrene with HNTs and sodium dodecyl sulfate (SDS) as the emulsifier [90] (Fig. 12). PAAm-HNTs hybrid hydrogel was also synthesized via free radical polymerization with acrylamide monomers and HNTs [72]. By utilizing nanostructure of HNTs to support hematin (a biomimetic catalyst) and inducing the aniline polymerization, HNTs-polyaniline (PANi) nanocomposites can be obtained [91] (Fig. 13).

4.2.4. Electrospinning

Electrospinning is a simple and versatile fiber synthesis technique in which a high-voltage electric field is applied to a stream of polymer solution, forming continuous micro/nanofibers. The electrospun fibers create a fabric network that has a high porosity, a very small pore

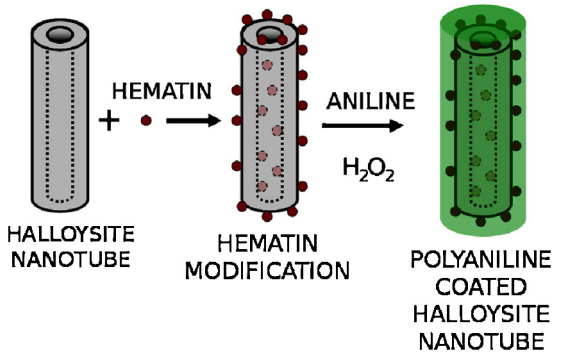

Fig. 13. Using HNTs as catalyst supporter for aniline polymerization.
Source: [91] Copyright 2010. Reproduced with permission from Elsevier Science Ltd., Oxford, UK.

Table 3
HNTs-polymer nanocomposites prepared by melt processing and the main properties enhancement (phr is the abbreviation of the parts per hundreds of rubber (or resin)).

Polymers	Instrument	HNTs loading	Focused main properties	Reference
LLDPE	Twin screw extruder	0–30 wt.%	Mechanical and flame-retardant property	[28]
PP	Twin screw extruder	0–30 wt.%	Thermal and mechanical properties	[27,32,64,98,113, 147,148]
PA 6	Twin screw extruder	0–30 wt.%	Thermal, mechanical and rheological properties	[23]
PLA	Single/twin screw extruder	0–30 phr	Thermal and mechanical properties	[73,110]
Poly (ε-caprolactone) (PCL)	Internal batch mixer (Haake rheocorder)	0–10 wt.%	Thermal, mechanical, and reological properties	[107]
Polyethersulfone (PES)	Water-assisted extrusion	0–16 wt.%	Thermal and flammability properties	[126]
NR	Two-roll mill	0–40 phr	Fatigue and hysteresis behavior, mechanical and thermal property	[74,149]
Ethylene-propylene-diene monomer (EPDM)	Two-roll mill	0–100 phr	Curing and tensile properties	[29,108,109,150]
Butadiene-acrylonitrile rubber (NBR)	Two-roll mill	5 phr	Flame-retardance property	[127]
NR-butadiene rubber blend	Intermeshing mixer	2.5 phr	Mechanical property	[47]
Fluoroelastomers (FKM)	Two-roll mill	0–30 phr	Mechanical, dynamic mechanical and thermal properties	[111]
Soy protein	Hot pressed instrument	0–10 wt. %	Mechanical properties and flammability	[128]
Wheatstarch	Twin screw extruder	0–8 wt.%	Thermal and mechanical properties	[116]
DNA	Ball milling	100 phr	Solubilization and dispersion	[151]

size, and a very large surface-to-volume ratio. Therefore, these materials could be used for many biomedical applications, such as drug delivery, artificial organs, wound dressing, and medical prostheses. The polymers used for electrospinning with HNTs range from PLA (or its copolymer or blend) to polyvinyl alcohol (PVA). Biodegradable PLA and PVA have good electrospinning properties, gaining them applications in many areas. Dichloromethane (DCM) or chloroform was employed to dissolve the PLA with dimethyl formamide (DMF) to enhance the electric conductivity. Water was used as a solvent for PVA. Mixing the HNTs with the polymer solution before spinning could generate composite nanofibers [92–97]. The morphology of the poly(lactic-co-glycolicacid) (PLGA) nanofibers does not change appreciably after incorporating HNTs, except that the mean diameter of the fibers increased with HNTs. From the TEM images of the HNTs-PLGA nanocomposite fibers (Fig. 14), the HNTs appear to be embedded in the fiber matrix and oriented along the fiber axis [94,97]. The coaxial alignment of HNTs within the PLGA nanofibers may be occur because the particle–particle interactions of the nanotubes can be overcome by the elongation and shear force imposed during the electrospinning process. HNTs could enhance the multifunctional properties of the polymer fiber mat, especially the mechanical properties and biocompatibility. Furthermore, drug-loaded HNTs could be mixed with PLGA for electrospinning, forming drug-loaded composite nanofibrous mats for various applications in tissue engineering and pharmaceutical sciences [92].

4.2.5. *Melt spinning*

HNTs can be melt spun with thermoplastics to prepare HNTs-polymer nanocomposite fibers. Lin et al. developed a master batch method to prepare HNTs-PP nanocomposite

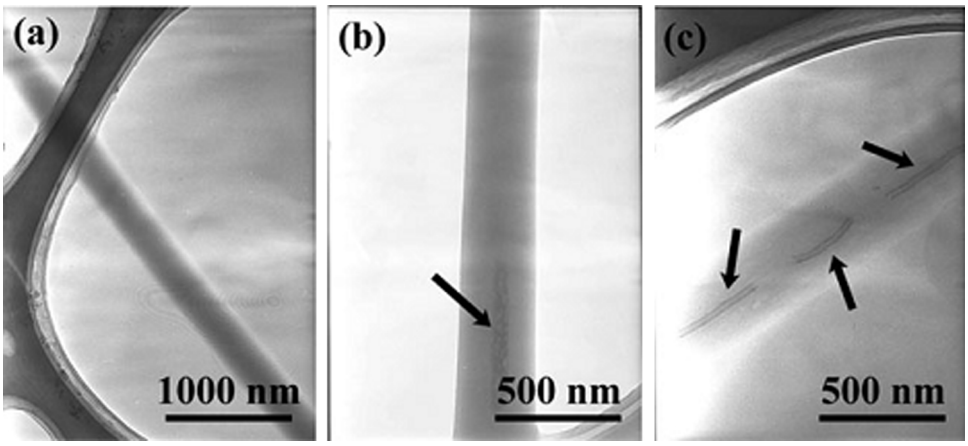

Fig. 14. TEM micrographs of (a) PLGA nanofibers, (b) HNTs-doped PLGA nanofibers with 5% HNTs relative to PLGA, and (c) CNTs-doped PLGA nanofibers with 5% CNTs relative to PLGA. The arrows indicate the nanotubes embedded within the PLGA nanofibers.
Source: [94] Copyright 2013. Reproduced with permission from of John Wiley & Sons, Inc., USA.

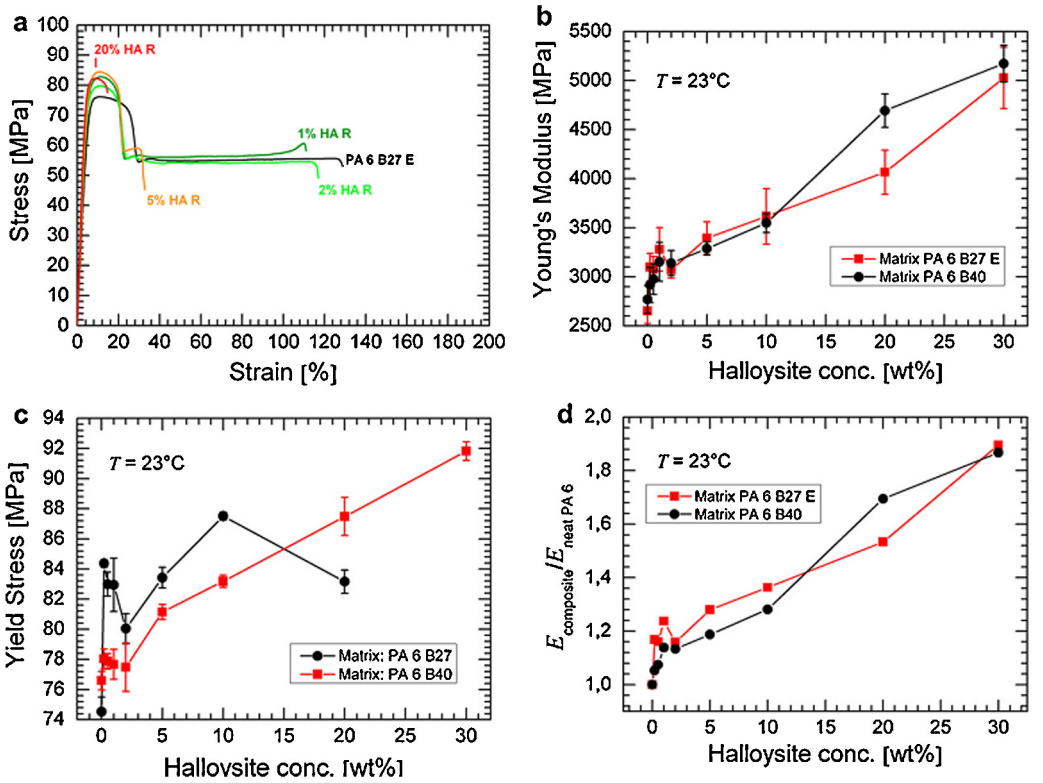

Fig. 15. Mechanical properties of the HNTs-PA6 nanocomposites: (a) representative curves of the tensile tests of the nanocomposites (nominal stress vs. nominal strain). (b) Young's modulus E. (c) Yield stress σ_y. (d) Reinforcement factor $E_{composite}/E_{neat\ PA\ 6}$ for the nanocomposites.
Source: [23] Copyright 2010. Reproduced with permission from Elsevier Science Ltd., Oxford, UK.

fibers with improved mechanical performance and spinability [98]. The spinability of the nanocomposite depended strongly on the HNTs loading. The maximum loading for the HNTs during spinning with PP was 1.5 wt.%. Above 1.5 wt.%, no continuous fibers could be obtained. The tensile strength of the HNTs-PP nanocomposite fibers was higher than the neat PP fiber. For 1 wt.% of HNTs, the breaking strength of the fiber increased 18.6%. This technology has been used industrially by Zhongshan Kecheng Chemical Fiber Co., LTD (China).

4.2.6. LbL technique

LbL deposition is a thin film fabrication technique. The films are formed by depositing alternating layers of oppositely charged materials with washing steps in between. LbL is an easy and inexpensive process for nano-architectures and allows a variety of materials to be incorporated within the films. HNTs are negatively charged; therefore, they can assemble via the LbL method with polycations, such as PEI [36], poly(allylaminehydrochloride) (PAH) [99–101], and chitosan [66,102]. Furthermore, drug or co-enzyme loaded HNTs can be incorporated within organic–inorganic composite films offering a novel method for fabricating core–shell nanomaterials with potential applications in drug release systems.

4.2.7. Electrophoretic deposition

Electrophoretic deposition (EPD) is an attractive method for depositing of polymer nanocomposite films toward biomedical applications. EPD is based on the electrophoretic motion of colloidal particles or polymer macromolecules under the influence of an electric field, forming a deposit at the electrode surface. EPD enables the fabrication of uniform films with a controlled thickness and offers many processing advantages, such as a high deposition rate, the possibility of deposition on substrates with complex shapes and the fabrication of composite films. Nanocomposite films containing HNTs and a polyelectrolyte (chitosan or hyaluronic acid) can be obtained using the cathodic and anionic deposition methods [103,104]. The polymers can be used as charging and dispersing agents for HNTs and hydroxyapatite (HA) in suspensions, as well as film forming agents for EPD with HNTs–HA-polymer nanocomposite films. The prepared nanocomposites have promising applications in biomedical implants with improved bioactivity, biocompatibility and corrosion protection for metallic implants.

5. Properties of HNTs-polymer nanocomposites

5.1. Mechanical reinforcement

The natural tubular morphology, nano-scale diameter, high aspect ratio and contrasting chemistry on external and internal surfaces of HNTs make them particularly attractive for reinforcing in polymer nanocomposites [17]. The improved mechanical properties are always attributed to the fact that the external load is efficiently transferred from

the polymer matrix to the HNTs. Most of the published work has focused on the enhanced mechanical properties of polymers induced by HNTs. The strength and modulus of HNTs-polymers were related to the nanotube loading, dispersion, and interfacial interactions in the systems.

5.1.1. HNTs loading

The HNTs loading strongly affects the reinforcement of polymer nanocomposites. The tensile properties of a HNTs-PA6 nanocomposite exhibited strong filler loading dependence (Fig. 15) [23]. The tensile strength and Young's modulus of PA6 increased with HNTs loading. The nanocomposites had twice the modulus of the neat PA6 when the HNTs content was 30 wt.%. Relative to PA6 with a different molecular weight, the HNTs showed a slightly different reinforcing effect. The mechanical properties, especially the modulus and hardness of the carboxylated butadiene–styrene rubber (xSBR), significantly increased after including the HNTs [85]. Not only does the ultimate stress increase with HNTs loading but also the modulus of the nanocomposites increases significantly with HNTs

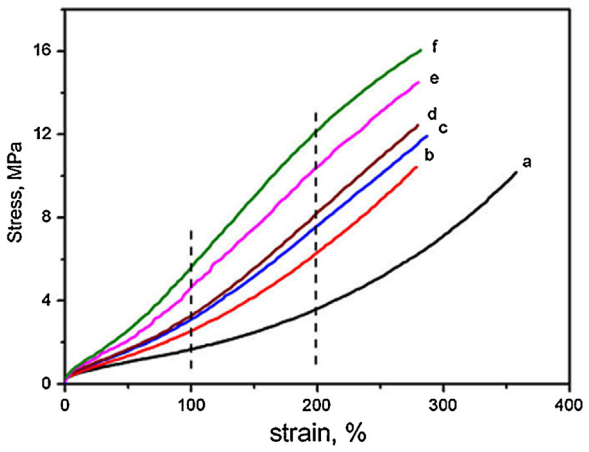

Fig. 16. Stress–strain curve of carboxylated butadiene–styrene rubber (xSBR) and HNTs–xSBR nanocomposites. (a) xSBR; (b) 2 phr HNTs; (c) 5 phr HNTs; (d) 10 phr HNTs; (e) 20 phr HNTs; (f) 30 phr HNTs.
Source: [85] Copyright 2008. Reproduced with permission from Elsevier Science Ltd., Oxford, UK.

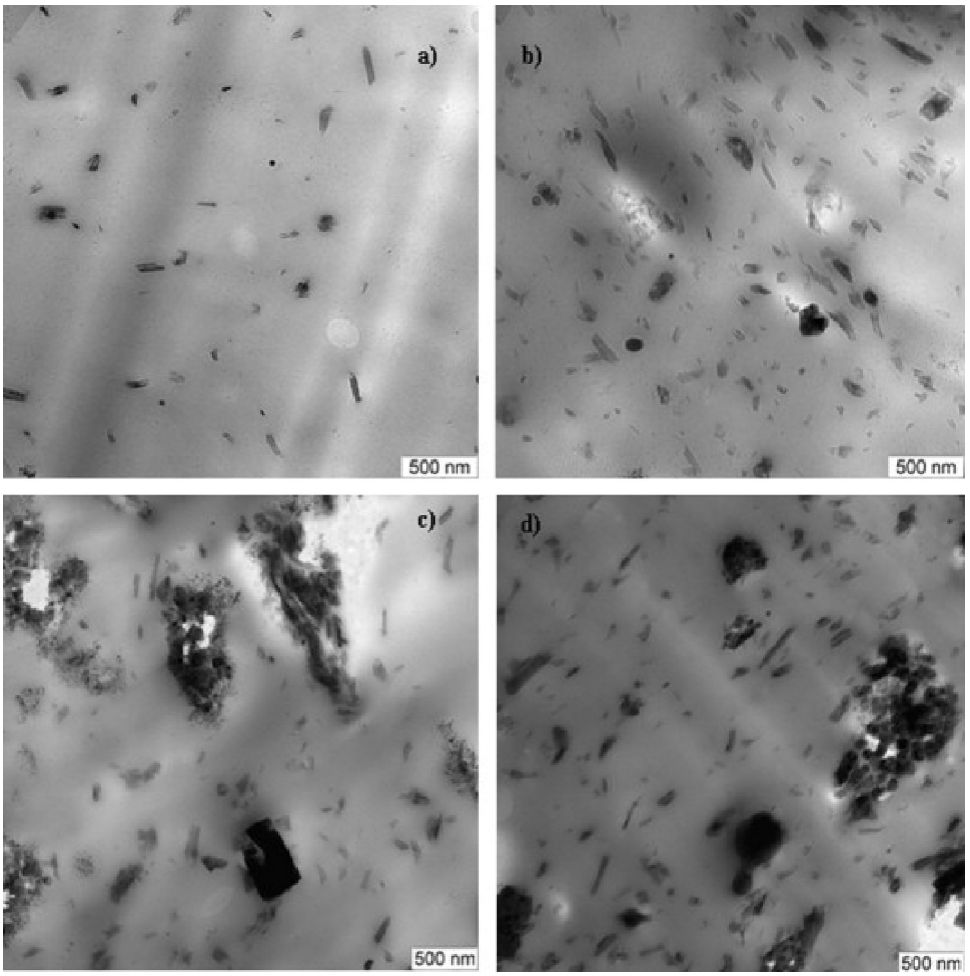

Fig. 17. TEM of (a) 5, (b) 10, (c) 20 and (d) 30 phr HNTs filled FKM.
Source: [111] Copyright 2011. Reproduced with permission from Elsevier Science Ltd., Oxford, UK.

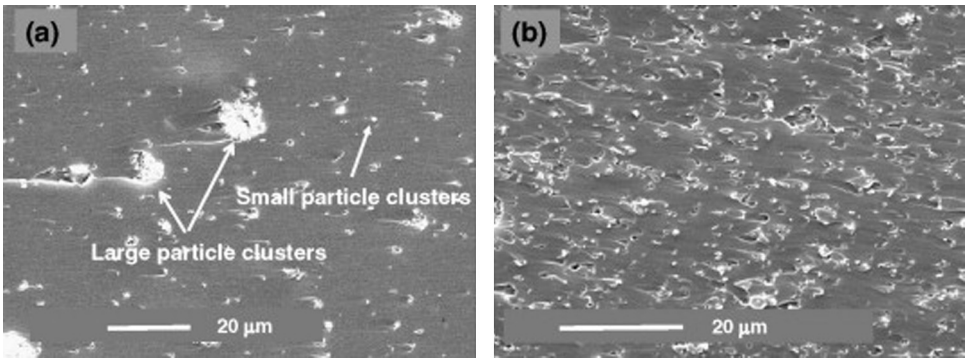

Fig. 18. Distribution of HNTs in HNTs–epoxy composites (10 wt.% HNTs) prepared by: (a) mechanical mixing and (b) ball milling homogenization.
Source: [112] Copyright 2009. Reproduced with permission from Elsevier Science Ltd., Oxford, UK.

loading (Fig. 16). When including only 5 phr of HNTs, the modulus at 100% elongation almost doubled compared to that of neat xSBR. With further increases in HNTs loading, the modulus of the HNTs–xSBR nanocomposites increased consistently. The impact strength of the HNTs–epoxy [86,105] and HNTs-vinyl-ester nanocomposites also increased significantly with the loading of HNTs. For instance, adding only 2.3 wt.% HNTs to the epoxy increased its impact strength by 4-fold (from 0.54 kJ/m^2 (neat epoxy) to 2.77 kJ/m^2). Moreover, the flexural properties were slightly increased by the HNTs. HNTs toughening was achieved at a much lower filler concentration compared to rubber or other nanoparticles (MMT or nano-TiO_2).

HNTs significantly improved both the tensile strength and Young's modulus of chitosan [78,106] and PVA [76] nanocomposite films. These mechanical properties were improved when loading of the HNTs up to 7.5 wt.%. The

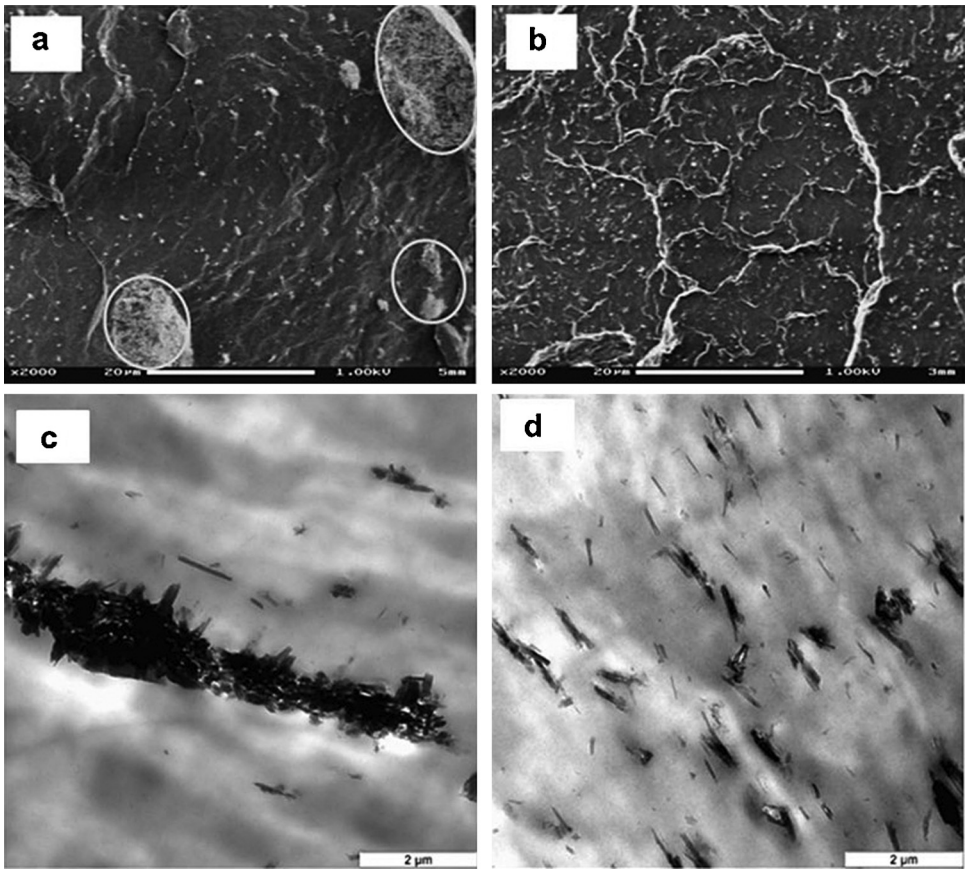

Fig. 19. SEM and TEM micrographs of PP/HNTs (92/8, weight ratio) ((a) and (c)) and water-assisted extruded PP/PP-g-Ma/HNTs (82.8/9.2/8 weight ratio) nanocomposite ((b) and (d)).
Source: [113] Copyright 2011. Reproduced with permission from Elsevier Science Ltd., Oxford, UK.

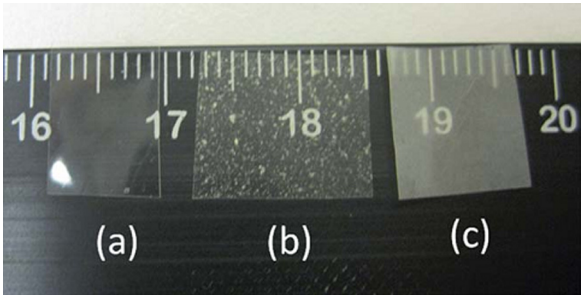

Fig. 20. Photograph of PVC films with different fillers: (a) PVC, (b) untreated Halloy-5, (c) St-Halloy-5. Large scale bar unit = cm.
Source: [52] Copyright 2011. Reproduced with permission from Royal Society of Chemistry, UK.

tensile strength, Young's modulus, and the elongation at break of PCL [107], PLGA nanofibers [92,94], EPDM [29,108,109] and FKM also improved after adding HNTs. For the HNTs-PLA bionanocomposites, their strength, modulus and toughness increased with increasing HNTs content [73,110].

5.1.2. Dispersion

The degree or uniformity of dispersion for the HNTs within polymers determines the final mechanical properties of nanocomposites. Although HNTs disperse better than other natural silicates (e.g., MMT and kaolinite) or CNTs, their ideal individual dispersion remains a challenge especially in nonpolar polymer matrixes or at high HNTs loading. The aggregated HNTs usually act as stress concentration points when fracturing the materials, deteriorating the mechanical properties. When the HNTs loading is low, they may be well dispersed. However, obtaining homogeneous dispersion at higher HNTs concentrations is difficult [78,87,88,111]. Fig. 17 demonstrates the state and the degree of dispersion for the HNTs in the FKM matrix as a function of the HNTs concentration. The dispersion of HNTs is hindered as their concentration increased.

To improve the dispersion of HNTs, many strategies have been developed. Ball mill homogenization and intercalated treatment were effective approaches that reduced the size of the HNTs clusters in an epoxy matrix (Fig. 18) [60,112]. After improving the HNTs dispersion in epoxies, the mechanical properties of the HNTs–epoxy nanocomposites were enhanced. Lecouvet et al. developed a water-assisted extrusion with a PP-graft-maleic anhydride (PP-g-MA) compatibilizer to prepare well dispersed HNTs-PP nanocomposites (Fig. 19) [113]. The better the dispersion of HNTs in PP was, the higher the storage modulus could be. By surface grating PBA, HNTs' dispersion and miscibility in the PVC matrix were improved (Fig. 20), leading to 65% increase in the E-modulus (compared with unmodified HNTs) [52]. Surface modified HNTs or the addition of a compatibilizer also can improve their dispersion in EPDM [108,109], PLA/PCL blends, and unsaturated polyesters. The modified HNTs have a much higher reinforcing ability than the raw HNTs. The coefficient of friction (C.O.F) for surface-treated HNTs-polyester nanocomposites was lower than that of the untreated composites due to the better dispersion of HNTs [88]. An interesting morphology (both

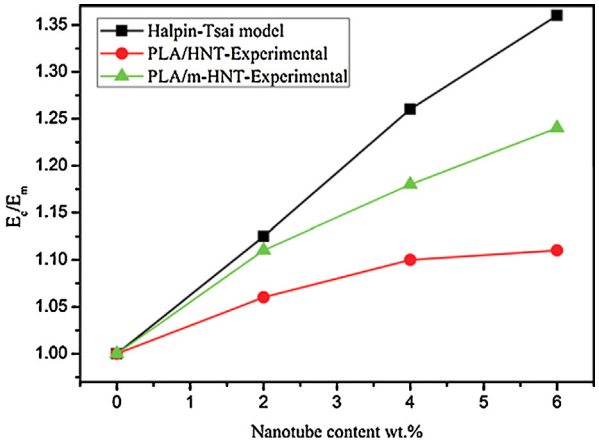

Fig. 21. Theoretical and experimental relative Young's modulus versus nanotube concentration for PLA/HNTs and PLA/m-HNTs nanocomposites.
Source: [110] Copyright 2013. Reproduced with permission from John Wiley & Sons, Inc., USA.

epoxy-rich region and HNTs-rich region) was observed in HNTs–epoxy resin nanocomposites [86]. This morphology was crucial for toughening the nanocomposites.

5.1.3. Interfacial bonding

The interfacial bonding between the HNTs and polymer matrix is also a critical factor for the enhancing mechanical properties of the nanocomposites. HNTs have intrinsic H-bond interactions or polar adsorption with polar polymers; therefore, the interface in the HNTs-polar polymers is usually satisfied [21,24,37,72,73,85,87,107,114]. However, the interfacial bonding should be strengthened for optimal reinforcement in HNTs-nonpolar polymer nanocomposites. Otherwise, the mechanical properties of HNTs-polymers will change little or even deteriorate after adding HNTs due to their huge polarity difference. For instance, the tensile strength of PVDF decreased when the HNTs concentration increased [83]. This decrease is caused by the weak interfacial adhesion between the PVDF matrix and the HNTs, facilitating debonding and slippage between the matrix and nanofillers.

As discussed above, surface pretreatments, such as grafting silanes or polymers, can modify the surface polarity and chemistry of HNTs and improve interfacial bonding. An alternative method for enhancing the interfacial interactions is incorporating compatibilizer [115]. These approaches can lead to a significant increase in mechanical properties. Quaternary ammonium salt treated HNTs have a better reinforcing effect on PLA than raw HNTs due to the increased interfacial bonding. The magnitude of the increases in the tensile strength and the Young's modulus were 29 and 25%, respectively, with 6 wt.% modified HNTs (Fig. 21) [110]. Benzoalkonium chloride-treated HNTs also imparted a better reinforcing effect to plasticized starch film compared to the unmodified HNTs due to the enhanced interfacial bonding [116]. Using electron transferring modifiers also increased the interfacial adhesion in the HNTs-non polar polymer nanocomposites. Examples of the electron-transferring modifiers included BBT [39,117], N-cyclohexyl-2-benzothiazole sulfonamide (CBS)

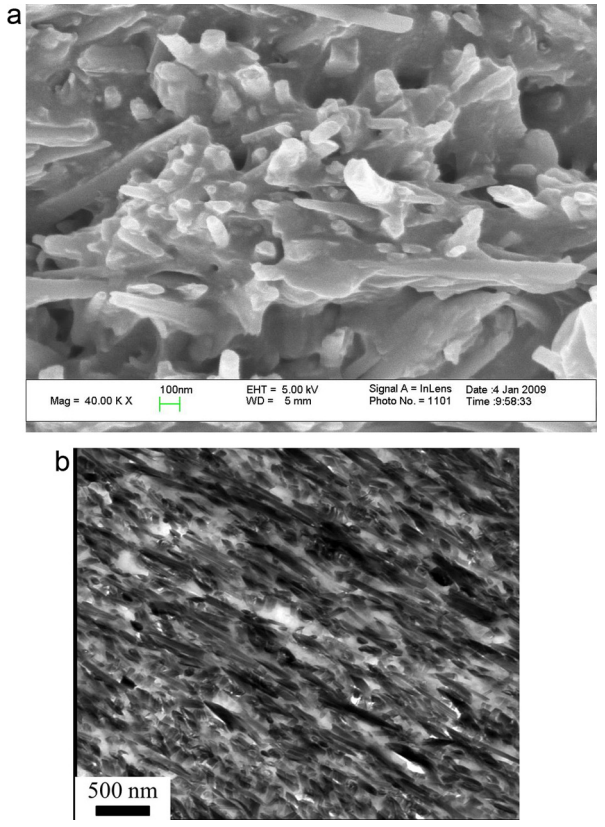

Fig. 22. SEM (a) and TEM (b) of the zinc disorbate modified HNTs-SBR (61 wt.% HNTs loading) nanocomposites.
Source: [119] Copyright 2010. Reproduced with permission from Taylor & Francis, London, UK.

[118], and EPB [63]. The tensile strength, flexural strength and flexural modulus of the HNTs-PP nanocomposites with BBT were 22%, 33% and 59% higher than those of the HNTs-PP without a modifier, respectively. An alternative route for enhancing the interfacial interactions was utilizing hydrogen bond interactions to construct inorganic–organic reinforcing networks in the polymer matrix. This effect could be achieved by adding melamine, diphenylguanine, 2,4,6-trimercapto-s-triazine, melamine cyanuric acid, tri-(2-hydroxyethyl)isocyanurate or β-cyclodextrin [64,65] to HNTs-polymer composites. The authors documented a major improvement in the tensile and flexural properties of PP composites with 30 wt.% HNTs.

Methacrylic acid or sorbic acid (SA) were added to HNTs-rubber nanocomposites to enhance the interfacial properties [119–121]. Unsaturated metal carboxylates, such as zinc dimethacrylate (ZDMA), zinc disorbate (ZDS) and magnesium dimethacrylate (MDMA), can be formed in-situ by reacting MMA or SA with ZnO or MgO. The metal carboxylate-modified HNTs-rubber nanocomposites exhibited highly increased mechanical strength, heat resistance and transparency. These improvements were ascribed to the strong interfacial interactions, including hydrogen bonding and complexation between the zinc salt and HNTs, confirmed by the continuous polymer residues on the nanotubes on the fractured surface (Fig. 22).

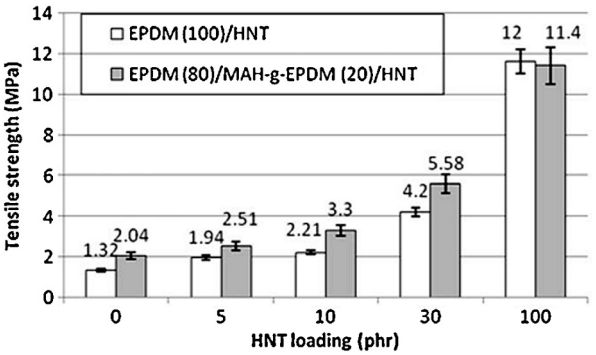

Fig. 23. Tensile strength of EPDM/HNTs and EPDM/MAH-g-EPDM/HNTs nanocomposites.
Source: [109] Copyright 2009. Reproduced with permission from Elsevier Science Ltd., Oxford, UK.

This strategy was effective for reinforcing NBR and SBR. MAH-g-EPDM compatibilized HNTs-EPDM nanocomposites showed much higher tensile properties compared than the un-compatibilized HNTs-EPDM nanocomposites (Fig. 23) due to the improved interfacial interactions between HNTs and EPDM in the presence of a compatibilizer [109].

5.2. Thermal stability

HNTs can increase the thermal stability of polymers for three reasons. First, HNTs have a much higher thermal stability than the polymers (HNTs begin to degrade at approximately 400 °C). Therefore, adding HNTs increases the thermal resistance of the polymers. Second, well-dispersed HNTs exert a barrier effect toward both mass and heat transports, improving the thermal stability of the nanocomposites. Third, the polymer chains and degradation products can enter the lumens of the HNTs, delaying mass transport and significantly improving the thermal stability. Enhancing the interfacial compatibility increased the thermal stability, because the polymer–filler interactions facilitated mass and heat transport in the nanocomposite. Du et al. investigated the thermal stability of HNTs-PP nanocomposites [32]. They found that adding 10 phr of modified HNTs could increase the temperature at 5% weight loss in nitrogen and the temperature at maximum weight loss rate in air by 60 °C and 74 °C, respectively. In another study, the onset temperature for the thermal degradation NR was improved by ~64 °C after adding 10 phr of modified HNTs, while the same amount of modified silica only led to 34 °C increase in the degradation temperature. HNTs can also significantly enhance the degradation temperature of PVA [44], PLA, VER [24], chitosan [78], EPDM [29], starch [116], and apple pectin [79]. However, in HNTs-hydroxypropyl cellulose (HPC) and HNTs-PEG nanocomposites films, the authors found that the t_d of the nanocomposites depended on the HNTs loading [80,81]. The presence of small amounts of HNTs caused thermal stabilization in polymer, while further additions enhanced the thermal degradation. The maximum value for t_d appears at ~20 wt.% HNTs content in the nanocomposites.

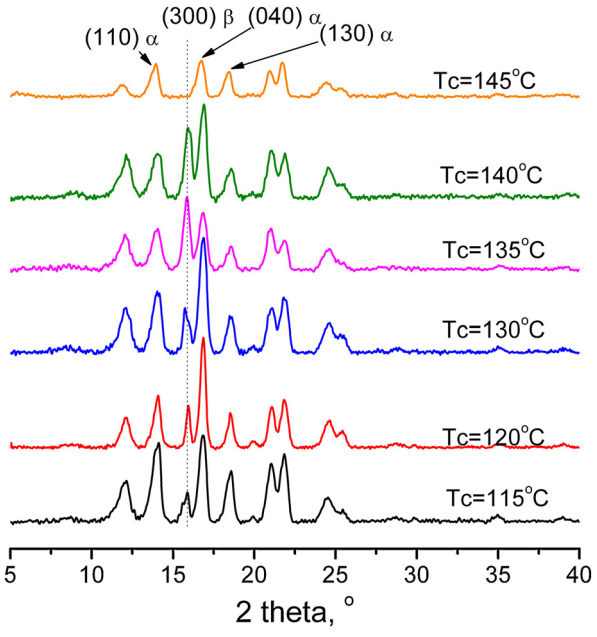

Fig. 24. XRD profiles of iPP/HNTs composite samples (20 phr HNTs) crystallized at the variable temperature.
Source: [123] Copyright 2009. Reproduced with permission from Elsevier Science Ltd., Oxford, UK.

5.3. Crystallization behavior

Generally, HNTs affect the crystallization of polymers by acting as heterogeneous nucleation points. The heterogeneous nucleation increases the nucleation and crystallization rates. Consequently, elevated crystallization temperatures, finer spherulites, higher crystallinities, and decreased activation energy for crystallization are observed. The changes in the crystallization behavior of a polymer that are caused by the incorporation of HNTs are related to the structural characteristics of HNTs and the interfacial interactions in the nanocomposites. HNTs act as the role of heterogeneous nucleating points for PVA [75,76], PLA [73,110], PP [122], PA6, PVDF [83], and PCL [107]. The crystallization temperature of the HNTs-PVA nanocomposite films fabricated by casting or coagulation initially increased with the HNTs loading. However, overloading with HNTs tended to decrease the improvement in the crystallization temperature [75]. The overloaded HNTs aggregated in the PVA matrix, decreasing their nucleating abilities due to the smaller specific surface area. Both the crystallization onset temperature and the crystallization peak temperature increased consistently with the HNTs content in a HNTs-PP nanocomposite prepared via solution mixing [122]. Meanwhile, the crystallinities of HNTs-PP nanocomposites were considerably higher than for neat PP. The cold crystallization peak for PLA (T_{cc}) shifted toward lower temperature after including HNTs [73]. Additionally, the crystallinities of the HNTs-PLA nanocomposites were substantially higher than for the neat PLA. The HNTs-PCL nanocomposites showed higher crystallization peak temperatures than neat PCL, and the crystallization temperature increased as the HNTs content increased [107]. However, the crystallinities of PCL were lowered in the nanocomposites compared to the neat PCL. The author attributed this to the decreased molecular mobility of the PCL chains in the nanocomposites, reducing the PCL crystal size and generating imperfections in the crystals.

Adding HNTs can alter the polymorphism of polymers, such as PP, PA6 and PVDF. The formation of polymorphisms in the HNTs-polymer nanocomposites was also related to the surface characteristics of the HNTs and the interfacial interactions with the polymers. The HNTs had a dual nucleating ability for α-iPP and β-iPP under the appropriate kinetic conditions [123]. The nanocomposite with 20 phr of HNTs had the highest β-iPP. The β-iPP content increased as the cooling rate decreased during non-isothermal crystallization. During isothermal crystallization, the β-crystal could be formed from 115 to 140 °C. The β-crystal content peaked 135 °C (Fig. 24). Furthermore, both α-phase crystals and γ-phase crystals were formed in the HNTs-PA6 nano-composites; only α-phase crystals were formed in neat PA6 [124]. The γ-phase crystal content of the PA6 nanocomposites increased with the HNTs loading. Additionally, adding HNTs promoted the crystallization of the γ-phase of PVDF [83]. The γ-phase content increased with the HNTs amount, peaked when the HNTs concentration was 10 phr, and sharply decreased afterward.

5.4. Flame retardance

Similar to most inorganic nanoparticles, HNTs can be used as an effective flame-retardant for polymers forming a thermally stable layer on the surface of the targeted material. Due to their tubular structure, HNTs can also form a spatial network that impedes the diffusion of thermal decomposition products toward flame and oxygen, delaying in mass transport and increasing flame resistance significantly. Similar to other inorganic nanoparticles, HNTs can catalyze the formation of a protective coat-like char of polymer, reducing heat release rate (HRR), due to their surface acidity [33,34]. Up to now, LLDPE [28], PP [32], PBT, ABS [125], PES [126], NBR [127], and soy protein [128] have been selected as polymer matrixes while investigate the effects of HNTs on flame resistance. From the cone calorimetric data, HNTs showed a decrease of flammability of the corresponding polymers significantly. The HRR, the specific extinction area (SEA), and the mass loss rate (MLR) of the nanocomposites were all substantially lower than those of neat polymer were. In addition, the HNTs extended the time needed to reach ignition and to burn out. Fig. 25 shows the typical heat release rate curves for the neat PBT and HNTs-PBT nanocomposites. Clearly, the HRR and SEA decreased with the incorporation of HNTs. Therefore, HNTs can be used a halogen-free flame-retardants for polymers without any sacrificing the mechanical properties. HNTs also had a synergetic effect with other halogen-free flame retardant compounds, such as antimony trioxide, magnesium hydroxide and melamine cyanurate, toward improving the flame retardance of rubber. Consequently, a self-extinguishing elastomeric material with good mechanical properties was obtained [127].

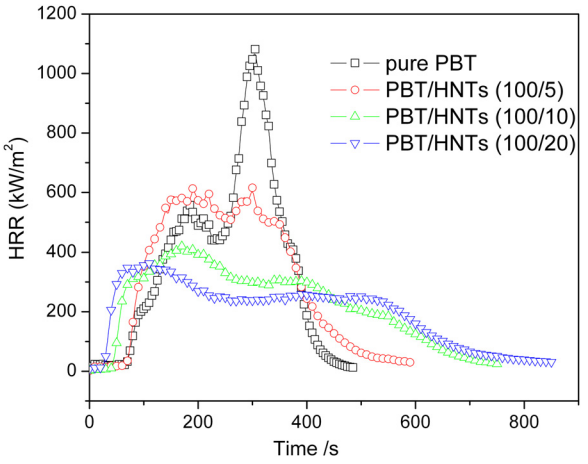

Fig. 25. The heat release rate curves for the neat PBT and PBT/HNTs nanocomposites (unpublished data).

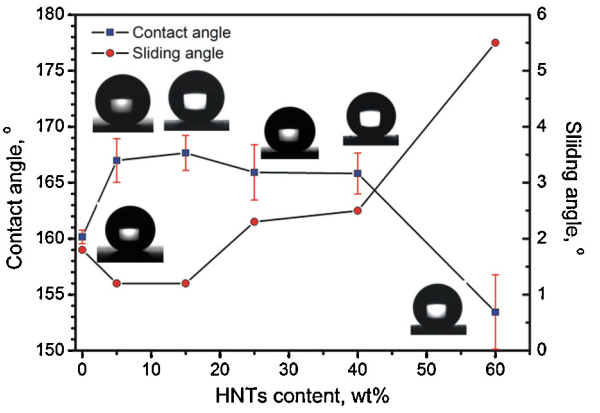

Fig. 26. Contact angles and sliding angles of the PP and PP/HNTs composite surfaces. (The inset shows the water drop shape on the corresponding composite surfaces).
Source: [122] Copyright 2010. Reproduced with permission from Elsevier Science Ltd., Oxford, UK.

5.5. Other properties

5.5.1. Coefficient of thermal expansion

Adding HNTs to polymers can lead to significant decrease in the CTE for epoxy resin and PA6. The CTE (25–100 °C) for the HNTs–epoxy hybrids with 12 wt.% HNTs was 19.6% lower than that of the neat epoxy resin [21]. In addition, the HNTs were competitive with the CTE performance of epoxy resins containing other nano-sized inorganics (silica, MMT, attapulgite). The CTE of PA6 can also be decreased by the incorporation of HNTs. The remarkable dimensional stability of the HNTs-polymer nanocomposite was related to the aluminosilicate nature of the HNTs and the interfacial interactions between the HNTs and the matrix.

5.5.2. Dielectric properties

The dielectric properties of polymer nanocomposites are interesting because they represent the ability to store/dissipate energy under exposure to an electric field. The dielectric properties are generally determined by monitoring the relaxation processes of the polymer chains and providing information about the molecular dynamics. Adding HNTs slightly affected both ε_r and σ at a certain frequency in the HPC film, remaining consistent with HNTs polar nature and the increased number of charge carriers in their presence [80]. The relaxation frequency at the maximum tan δ (ν_{max}) also changes slightly at 20 wt.% HNTs; afterward, this value sharply decreases upon HNTs addition, suggesting reduced local polymer chain mobility occurs in the presence of the nanotubes.

5.5.3. Wettability properties

The surface wettability of a material is important for many applications, and the wettability is usually determined using the contact angle method. The contact angle is related to the surface roughness and the chemical composition. HNTs are hydrophilic, exhibiting a 10° water contact angle. Interestingly, adding HNTs to polymers led to completely different changes in the wettability of the surface.

HNTs were incorporated into PP to tailor the surface wettability of the solution–cast nanocomposites [122]. Without HNTs, PP could form rough surface with a water contact angle of approximately 160°. The contact angles increased when less than 60 wt.% HNTs were present in the composites (Fig. 26). The maximum contact angle for the HNTs-PP nanocomposites was close to 170° with 15 wt.% HNTs due to the changes in surface microstructures of the nanocomposites caused by HNTs via their nucleation effect while drying of the nanocomposites. However, for the HNTs-pectin and HNTs-PCL nanocomposites, the water contact angle decreased after adding HNTs due to the increased surface hydrophilicity caused by the HNTs at the interface [80,107]. For the HNTs-HPC nanocomposite films, an increased water contact angle was found at 15 wt.% HNTs due to a rearrangement of the polymer structure that exposed the hydrophobic moieties to the interface after an interaction with the inner HNTs layer [80].

5.5.4. Self-healing properties

HNTs have empty lumens that can be loaded with corrosion inhibitors. Additionally, HNTs are easily dispersed in thermosetting resins and are environmental-friendly materials. These features make HNTs a candidate for self-healing anticorrosion coating formulations [101,129–131]. Abdullayev et al. prepared polyurethane and acrylic paints doped with HNTs loaded with benzotriazole, 2-mercaptobenzimidazole, and 2-mercaptobenzothiazole corrosion inhibitors, generating a self-healing nanocomposite coating for copper (Fig. 27) [131]. The inhibitors could be kept in the tubes buried in polymeric paint layer for long period and the release was enhanced in the coating defects exposed to humid media over 20–50 h; this interval was sufficient for the protective layer formation.

6. Biomedical applications of HNTs-polymers nanocomposites

The environmental friendliness, biocompatibility, and natural abundance make HNTs an important nanomaterial

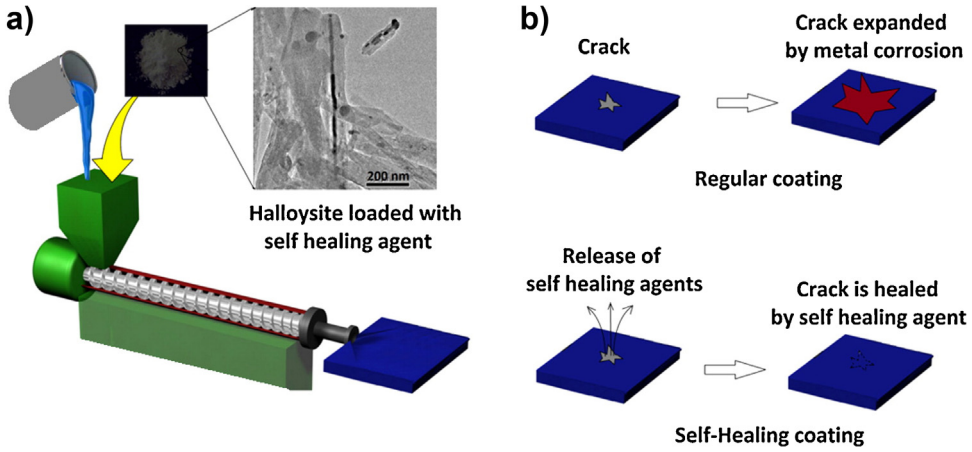

Fig. 27. (a) Preparation of HNTs-polymeric coating and (b) the behaviors of the regular and self-healing coatings in corrosion process. *Source:* [131] Copyright 2013. Reproduced with permission from American Chemical Society, Washington DC, USA.

for developing biomedical applications. Up to now, the HNTs-polymer nanocomposites are applicable in tissue engineering scaffolds, drug delivery, cancer cell isolation, bone implant and cosmetic.

6.1. Tissue engineering scaffold

Tissue engineering scaffolds are structures made of artificial or natural substances used to shape cells growth. In general, these scaffolds should be porous, cyto- and tissue compatible, bioactive, and mechanically strong. HNTs have been added to biodegradable polymers, such as PVA [76], chitosan [106], PLA [132], and PLGA [92,96] to prepare tissue engineering scaffolds. HNTs-reinforced PVA bionanocomposite films are highly compatible with the osteoblast and fibroblast cells [76]. The HNTs-chitosan nanocomposite scaffolds exhibited a significant enhancement in compressive strength, compressive modulus, and thermal stability compared with the pure chitosan scaffold. Meanwhile, the HNTs-chitosan nanocomposite scaffolds exhibited a highly porous structure; the HNTs had little effect on the pore structure and porosity of the chitosan scaffolds. Mouse fibroblasts could develop on the HNTs–chitosan nanocomposites surfaces, even at 80 wt.% HNTs. Electrospun HNTs-PLGA nanofibrous mats have excellent biocompatibility [92]. An MTT proliferation assay showed that the incorporation of HNTs did not significantly influence the cell proliferation or viability compared to the pure PLGA fibers. The SEM observations of the cell morphology showed that the HNTs-PLGA nanofibrous scaffolds could provide a three-dimensional structure with interconnected pores for cell attachment and migration. The fibroblast cells cultured on the nanocomposite scaffolds displayed a phenotypic shape, suggesting that the cells could penetrate and migrate within the scaffolds similar to native extracellular matrix. Therefore, the HNTs-polymer nanocomposites exhibited great potential for applications in tissue engineering.

6.2. Drug/DNA carrier

The potential applications of HNTs as a drug delivery vehicles were widely reported in literature [25,133–137], and the drug release rate could be slowed further by coating polymers onto the drug-loaded HNTs [66,77,138]. In addition, the HNTs were reportedly biocompatible. Therefore, HNTs-polymer nanocomposites are promising drug containers [6,139]. The drug-loaded HNTs-polymer nanocomposites are a formulation including powders, suspensions, and a fibrous scaffold, with many potential applications in drug/DNA delivery.

A slow release was observed for diltiazem hydrochloride, 5-aminosalicylic acid, tetracycline, and propanol hydrochloride entrapped within the lumen as well as sites on the external surfaces of the HNTs. The HNTs were mixed with a saturated solution of the drugs in water, ethanol, acetone, or other solvents and exposed to high vacuum. Typical HNTs have a lumen volume of ca. 10 vol.%; therefore, the loading abilities of HNTs are limited. The selective etching of alumina from the inside of the tubes was explored, increasing the lumen capacity by 2–3 times and enable additionally sustained drugs release [69]. To enhance their capacity toward hydrophobic drugs, phosphonic acid was bound to the alumina sites in the tube lumen [35]. Coating PVA on the HNTs can delay diphenhydramine hydrochloride release [77]. Additionally, the chitosan- and PEI-coated HNTs show a dramatically reduced release compared to the uncoated HNTs [66,138]. For example, on day 9, the uncoated HNTs had released 88% of their final drug payload, while the coated HNTs released only 78% of their total drug load (Fig. 28). After 20 days the drug release rate was very slow for the chitosan coated HNTs, involving no more than 10% content of the loaded drug. The drugs embedded in the lumen was released lowly because they must diffuse outward through the pores of the tubes before traveling through the narrow lumen to reach the open ends. The drug release was further hindered by the chitosan coating on the surface of the HNTs, providing an additional barrier through

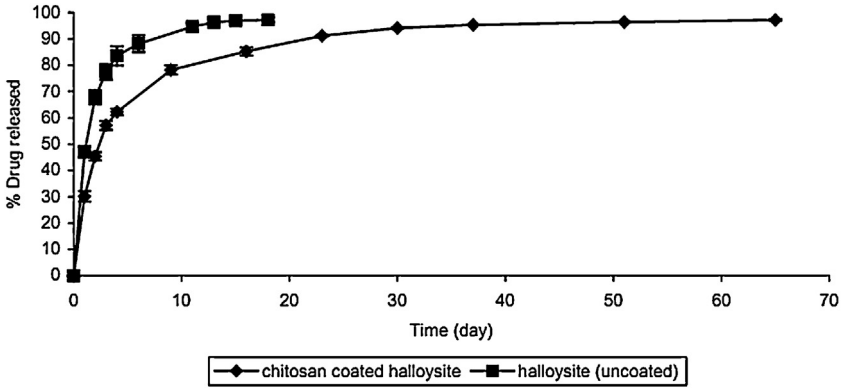

Fig. 28. Release of tetracycline base from HNTs (uncoated) and HNTs coated with chitosan into buffer pH 6.8 at 37 °C.
Source: [66] Copyright 2004, Reproduced with permission from Elsevier Science Ltd., Oxford, UK.

which the drug must diffuse. Apart from drugs, other active agents, such as self-healing [131], anticorrosion [101,130], and antimicrobial agents, as well as proteins, and DNA [140], can also be loaded for sustained release. Very recently, the advances in HNTs-polymer nanocomposites toward sustained release have been reviewed by Lvov et al. [6,139].

6.3. Cancer cell isolation

Streamlining the separating of cancer cells from patient blood is important for the development of individualized treatments for cancer. HNTs were coated with a layer of poly-L-lysine on their surfaces and then functionalized with recombinant human selectin protein. This method can increase the capture ability of HNTs toward leukemic cells under flow. Therefore, this effective and practical route for enhancing cancer cell capture ultimately promises to advance the feasibility of individualized cancer treatment [141].

6.4. Bone implants

A bone implant or bone graft is a medical procedure in which a damaged or missing piece of bone is replaced with a graft. Common bone implants commonly include dental implants and devices used to repair chipped, broken, or severely damaged bones. PMMA bone cement has good biocompatibility and mechanical properties, explaining its use during orthopedic repair specifically in joint replacement arthroplasty. By using the lumen of HNTs, gentamicin, which is a antibiotic, was loaded in to the tubes by Wei et al. [142]. Afterward, the drug loaded HNTs were mixed with PMMA to form bone cement. The PMMA/HNTs/gentamicin composite provided sustained release for up to 300–400 h with enhanced release behavior at the cement cracks and comparable strength and moduli to the pure PMMA cement. Another advantage of the ternary composites was that their adhesion to bone was significantly increased. Due to the good mechanical properties and biocompatibility of the biodegradable PLA-HNTs composites they have potential applications as bone implants [143].

6.5. Cosmetic applications

Due to their strong absorption abilities, HNTs can be used as a cleansing mask that deeply purifies and refines facial pores. For example, the main active ingredient of the Living Nature Deep Cleansing Mask is halloysite from New Zealand. More importantly, the hollow HNTs tube can be filled with various active ingredients including those used for cosmetics, household and personal care products, and as well as other agents that could benefit from extended release. Suh et al. investigated the possibility of HNTs using a nanocontainer during the loading and extended release of glycerol for cosmetic applications [144]. The tubes showed no toxic effect against the fibroblast and breast cancer cells over 48 h. The total elapsed time for the glycerol release from the nanotubes exceeded 20 h. Coating with several alternate layers of PEI and polyacrylic acid (PAA) could further retard the glycerol release rate.

7. Conclusion and future prospects

In this review, we provided an overview of the recent research regarding HNTs-polymer nanocomposites and insights into the factors that ultimately control the properties of nanocomposite. The following points are evident for the HNTs-polymer nanocomposites:

(1) A novel 1D natural nanomaterial called HNTs have a unique combination of tubular structure, large aspect ratio, natural availability, rich functionality, good biocompatibility, and high mechanical strength. These characteristics result in exceptional mechanical, thermal, and biological properties at a low price for HNTs-polymer nanocomposites. Therefore, HNTs are promising nanoparticles for high-performance polymer composites and multi-function nanocomposites.
(2) Apart from the nature of the HNTs, the dispersion state and the interfacial interactions are two critical factors that determine the properties of polymer nanocomposites. Functionalizing nanotubes is extremely important for their processing and applications regarding the enhancement of the mechanical, thermal, and biological properties of the polymer composites. The covalent

and non-covalent functionalization of HNTs each has its respective advantages; the functionalization method should be selected based on the type of polymer matrix and the cost of the methods.

(3) HNTs can be mixed with almost every polymer using the most common instruments and approaches. During processing, HNTs have a preferred orientation in polymer matrix when under shear force. The processing approaches for HNTs-polymer nanocomposites include solution mixing, melt processing, in situ polymerization, melt spinning, electrospinning, and the layer-by-layer technique. The key for processing is achieving a good dispersion of the nanotubes and good interfacial interactions between the HNTs and the polymers.

(4) The HNTs-polymer nanocomposites exhibit substantially increased mechanical, thermal, and flame retardant properties. Additionally, these materials have unique crystallization behaviors. The filler concentration, the dispersion state, and the interfacial adhesion affect the polymer reinforcement, as has been discussed in detail. To optimize the reinforcing effect, the interfacial bonding must be designed according to the unique traits of the HNTs.

(5) HNTs-polymer nanocomposites show good biocompatibility and sustained drug sustained release abilities, therefore, these materials are promising for tissue engineering and as drug vehicles. Additionally, the other biomedical applications of HNTs-polymers, such as cancer diagnose/treatment, wound dressing, and biosensing, should be developed. The biological effect and the toxicology of HNTs should also be thoroughly investigated.

The significant progress toward the synthesis, structural characterization, and understanding the properties of HNTs-polymer nanocomposites made in the past several years points toward a bright future. The potential applications of the HNTs-polymer nanocomposites include high performance plastics for use in structural and packing materials, flame retardant rubber/coatings, and biocompatible materials, such as tissue engineering scaffold and drug delivery vehicle. However, the large-scale utilization of HNTs for preparing high performance and multifunctional polymer nanocomposites with a low cost has not yet been realized due to the inhomogeneous quality of the natural raw HNTs and the weak interfacial interactions of the nanocomposite systems. However, some companies (i.e., Applied Minerals Inc., USA and Natural Nano, Inc., USA) have industrialized HNTs-polymer nanocomposite products. The applied polymers include PP, PE and PA6. The following urgent works regarding HNTs-polymer nanocomposites should include the development of chemical synthetic methods for HNTs that accurately control their dimension, studying the properties and reaction mechanism of the composites via computer simulation, systemic evaluation of the in vivo toxicity and biodegradation behavior of the HNTs, and exploring the possibility for their use during energy storage and transformation. Finally, we anticipate that breakthroughs in the research and development for HNTs-polymer nanocomposite will appear in high performance nanocomposites for the aircraft/automotive industries, environment protection, and biomedical materials.

Acknowledgements

This work was financially supported by the Guangdong Natural Science Funds for Distinguished Young Scholar (Grant No. S2013050014606), the Joint Funds of the National Natural Science Foundation of China and Guangdong Province (Grant No. U1134005), the project of regional demonstration for Guangdong Ocean Economic Innovative Development (Grant No. GD2012-B03-009), the National Natural Science Foundation of China (Grant No. 51003031), the Research Fund for the Doctoral Program of Higher Education of China (Grant No. 20114401120003), and the Key Project of Department of Education of Guangdong Province (Grant No. cxzd1108). The authors also thank Dr. Hau-To Wong for reading and revising of the manuscript.

References

[1] Sinha Ray S, Okamoto M. Polymer/layered silicate nanocomposites: a review from preparation to processing. Prog Polym Sci 2003;28:1539–641.
[2] Moniruzzaman M, Winey KI. Polymer nanocomposites containing carbon nanotubes. Macromolecules 2006;39:5194–205.
[3] Byrne MT, Gun'ko YK. Recent advances in research on carbon nanotube-polymer composites. Adv Mater 2010;22:1672–88.
[4] Joussein E, Petit S, Churchman J, Theng B, Righi D, Delvaux B. Halloysite clay minerals – a review. Clay Miner 2005;40:383–426.
[5] Du M, Guo B, Jia D. Newly emerging applications of halloysite nanotubes: a review. Polym Int 2010;59:574–82.
[6] Lvov Y, Abdullayev E. Functional polymer–clay nanotube composites with sustained release of chemical agents. Prog Polym Sci 2013;38:1690–719.
[7] Berthie P. Analyse de l'halloysite. Ann Chim Phys 1826;32:332–5.
[8] Macewan DMC. The nomenclature of the halloysite minerals. Miner Mag 1947;28:36–44.
[9] Brindley GW, Robinson K, MacEwan DMC. The clay minerals halloysite and meta-halloysite. Nature 1946;157:225–6.
[10] Mcdowall IAN, Vose W. Sedimentation of halloysite. Nature 1952;170:368.
[11] Macewan DMC. Halloysite–organic complexes. Nature 1946;157:159–60.
[12] Brindley GW, Robinson K, Goodyear J. X-ray studies of halloysite and metahalloysite. Miner Mag 1948;28:407–22.
[13] Hendricks SB. Crystal structures of the clay mineral hydrates. Nature 1938;142:38.
[14] Mehmel M. Uber die struktur von halloysit und metahalloysit. Zeits Krist 1935;90:35–43.
[15] Askenasy PE, Dixon JB, McKee TR. Spheroidal halloysite in a Guatemalan soil. Soil Sci Soc Am J 1974;37:799–803.
[16] Singh B. Why does halloysite roll? – A new model. Clays Clay Miner 1996;44:191–6.
[17] Pasbakhsh P, Churchman GJ, Keeling JL. Characterisation of properties of various halloysites relevant to their use as nanotubes and microfibre fillers. Appl Clay Sci 2013;74:47–57.
[18] Lecouvet B, Horion J, Haese CD, Bailly C, Nysten B. Elastic modulus of halloysite nanotubes. Nanotechnology 2013;24, 105704/1-8.
[19] Lu D, Chen H, Wu J, Chan CM. Direct measurements of the Young's modulus of a single halloysite nanotube using a transmission electron microscope with a bending stage. J Nanosci Nanotechnol 2011;11:7789–93.
[20] Guimaraes L, Enyashin AN, Seifert G, Duarte HA. Structural, electronic, and mechanical properties of single-walled halloysite nanotube models. J Phys Chem C 2010;114:11358–63.
[21] Liu MX, Guo BC, Du ML, Cai XJ, Jia DM. Properties of halloysite nanotube–epoxy resin hybrids and the interfacial reactions in the systems. Nanotechnology 2007;18, 455703/1-9.

[22] Anonymous. Halloysite mineral data; 2014. http://webmineral.com/data/Halloysite.shtml [accessed January 2014].
[23] Handge UA, Hedicke-Hochstotter K, Altstadt V. Composites of polyamide 6 and silicate nanotubes of the mineral halloysite: influence of molecular weight on thermal, mechanical and rheological properties. Polymer 2010;51:2690–9.
[24] Alhuthali A, Low IM. Water absorption, mechanical, and thermal properties of halloysite nanotube reinforced vinyl-ester nanocomposites. J Mater Sci 2013;48:4260–73.
[25] Price RR, Gaber BP, Lvov Y. In-vitro release characteristics of tetracycline HCl, khellin and nicotinamide adenine dineculeotide from halloysite; a cylindrical mineral. J Microencapsulation 2001;18:713–22.
[26] Shchukin DG, Sukhorukov GB, Price RR, Lvov YM. Halloysite nanotubes as biomimetic nanoreactors. Small 2005;1:510–3.
[27] Du M, Guo B, Wan J, Zou Q, Jia D. Effects of halloysite nanotubes on kinetics and activation energy of non-isothermal crystallization of polypropylene. J Polym Res 2010;17:109–18.
[28] Jia Z, Luo Y, Guo B, Yang B, Du M, Jia D. Reinforcing and flame-retardant effects of halloysite nanotubes on LLDPE. Polym Plast Technol Eng 2009;48:607–13.
[29] Ismail H, Pasbakhsh P, Fauzi MNA, Abu Bakar A. Morphological, thermal and tensile properties of halloysite nanotubes filled ethylene propylene diene monomer (EPDM) nanocomposites. Polym Test 2008;27:841–50.
[30] Ismail H, Salleh SZ, Ahmad Z. Properties of halloysite nanotubes-filled natural rubber prepared using different mixing methods. Mater Des 2013;50:790–7.
[31] Xie XL, Mai YW, Zhou XP. Dispersion and alignment of carbon nanotubes in polymer matrix: a review. Mater Sci Eng R 2005;49:89–112.
[32] Du ML, Guo BC, Jia DM. Thermal stability and flame retardant effects of halloysite nanotubes on poly(propylene). Eur Polym J 2006;42:1362–9.
[33] Qin H, Zhang S, Zhao C, Hu G, Yang M. Flame retardant mechanism of polymer/clay nanocomposites based on polypropylene. Polymer 2005;46:8386–95.
[34] Wei P, Tian G, Yu H, Qian Y. Synthesis of a novel organic–inorganic hybrid mesoporous silica and its flame retardancy application in PC/ABS. Polym Degrad Stab 2013;98:1022–9.
[35] Yah WO, Takahara A, Lvov YM. Selective modification of halloysite lumen with octadecylphosphonic acid: new inorganic tubular micelle. J Am Chem Soc 2012;134:1853–9.
[36] Lvov Y, Price R, Gaber B, Ichinose I. Thin film nanofabrication via layer-by-layer adsorption of tubule halloysite, spherical silica, proteins and polycations. Colloids Surf A 2002;198–200:375–82.
[37] Liu MX, Zhang Y, Wu CC, Xiong S, Zhou CR. Chitosan/halloysite nanotubes bionanocomposites: structure, mechanical properties and biocompatibility. Int J Biol Macromol 2012;51:566–75.
[38] Solomon DH. Clay minerals as electron acceptors and/or electron donors in organic reactions. Clays Clay Miner 1968;16:31–9.
[39] Liu MX, Guo BC, Zou QL, Du ML, Jia DM. Interactions between halloysite nanotubes and 2,5-bis(2-benzoxazolyl) thiophene and their effects on reinforcement of polypropylene/halloysite nanocomposites. Nanotechnology 2008;19, 205709/1-10.
[40] Wang AP, Kang FY, Huang ZH, Guo ZC, Chuan XY. Synthesis of mesoporous carbon nanosheets using tubular halloysite and furfuryl alcohol by a template-like method. Microporous Mesoporous Mater 2008;108:318–24.
[41] Wilson IR. Kaolin and halloysite deposits of China. Clay Miner 2004;39:1–15.
[42] Wilson IR, Santos HD, Santos PD. Kaolin and halloysite deposits of Brazil. Clay Miner 2006;41:697–716.
[43] Patterson SH, Murray HH. Kaolin, refractory clay, ball clay, and halloysite in North America, Hawaii, and the Caribbean region. In: USGS Professional Paper 1306. 1984. p. 56.
[44] Qiu K, Netravali AN. Halloysite nanotube reinforced biodegradable nanocomposites using noncrosslinked and malonic acid crosslinked polyvinyl alcohol. Polym Compos 2013;34:799–809.
[45] Ames LL, Sand LB. Halloysite formed in a calcareous hot-spring environment. Clays Clay Miner 1957;6:378–85.
[46] García FJ, García Rodríguez S, Kalytta A, Reller A. Study of natural halloysite from the dragon mine Utah (USA). Z Anorg Allg Chem 2009;635:790–5.
[47] Poikelispää M, Das A, Dierkes W, Vuorinen J. Synergistic effect of plasma-modified halloysite nanotubes and carbon black in natural rubber–butadiene rubber blend. J Appl Polym Sci 2013;127:4688–96.
[48] Yuan P, Southon PD, Liu Z, Green MER, Hook JM, Antill SJ, Kepert CJ. Functionalization of halloysite clay nanotubes by grafting with γ-aminopropyltriethoxysilane. J Phys Chem C 2008;112:15742–51.
[49] Liu MX, Guo BC, Du ML, Lei YD, Jia DM. Natural inorganic nanotubes reinforced epoxy resin nanocomposites. J Polym Res 2008;15:205–12.
[50] Guo B, Zou Q, Lei Y, Jia D. Structure and performance of polyamide 6/halloysite nanotubes nanocomposites. Polym J 2009;41:835–42.
[51] Joo Y, Jeon Y, Lee SU, Sim JH, Ryu J, Lee S, Lee H, Sohn D. Aggregation and stabilization of carboxylic acid functionalized halloysite nanotubes (HNT—COOH). J Phys Chem C 2012;116:18230–5.
[52] Yin B, Hakkarainen M. Core–shell nanoparticle-plasticizers for design of high-performance polymeric materials with improved stiffness and toughness. J Mater Chem 2011;21:8670–7.
[53] Zhang J, Zhang D, Zhang A, Jia Z, Jia D. Poly (methyl methacrylate) grafted halloysite nanotubes and its epoxy acrylate composites by ultraviolet curing method. J Reinf Plast Compos 2013;32:713–25.
[54] Liu C, Luo YF, Jia ZX, Zhong BC, Li SQ, Guo BC, Jia DM. Enhancement of mechanical properties of poly(vinyl chloride) with polymethyl methacrylate-grafted halloysite nanotube. Express Polym Lett 2011;5:591–603.
[55] Li C, Liu J, Qu X, Guo B, Yang Z. Polymer-modified halloysite composite nanotubes. J Appl Polym Sci 2008;110:3638–46.
[56] Li C, Liu J, Qu X, Yang Z. A general synthesis approach toward halloysite-based composite nanotube. J Appl Polym Sci 2009;112:2647–55.
[57] Yah WO, Xu H, Soejima H, Ma W, Lvov Y, Takahara A. Biomimetic dopamine derivative for selective polymer modification of halloysite nanotube lumen. J Am Chem Soc 2012;134:12134–7.
[58] Liu Y, Cai Q, Li H, Zhang J. Fabrication and characterization of mesoporous carbon nanosheets using halloysite nanotubes and polypyrrole via a template-like method. J Appl Polym Sci 2013;128:517–22.
[59] Guimarães JL, Peralta-Zamora P, Wypych F. Covalent grafting of phenylphosphonate groups onto the interlamellar aluminol surface of kaolinite. J Colloid Interface Sci 1998;206:281–7.
[60] Tang Y, Deng S, Ye L, Yang C, Yuan Q, Zhang J, Zhao C. Effects of unfolded and intercalated halloysites on mechanical properties of halloysite–epoxy nanocomposites. Compos Part A 2011;42:345–54.
[61] Jing H, Higaki Y, Ma W, Wu H, Yah WO, Otsuka H, Lvov YM, Takahara A. Internally modified halloysite nanotubes as inorganic nanocontainers for a flame retardant. Chem Lett 2013;42:121–3.
[62] Solomon D, Rosser M. Reactions catalyzed by minerals: Part I. Polymerization of styrene. J Appl Polym Sci 1965;9:1261–71.
[63] Liu M, Guo B, Du M, Jia D. The role of interactions between halloysite nanotubes and 2,2-(1,2-ethenediyldi-4,1-phenylene) bisbenzoxazole in halloysite reinforced polypropylene composites. Polym J 2008;40:1087–93.
[64] Du ML, Guo BC, Liu MX, Jia DM. Formation of reinforcing inorganic network in polymer via hydrogen bonding self-assembly process. Polym J 2007;39:208–12.
[65] Du M, Guo B, Liu M, Cai X, Jia D. Reinforcing thermoplastics with hydrogen bonding bridged inorganics. Physica B 2010;405:655–62.
[66] Kelly HM, Deasy PB, Ziaka E, Claffey N. Formulation and preliminary in vivo dog studies of a novel drug delivery system for the treatment of periodontitis. Int J Pharm 2004;274:167–83.
[67] Lvov Y, Aerov A, Fakhrullin R. Clay nanotube encapsulation for functional biocomposites. Adv Colloid Interface Sci 2013, http://dx.doi.org/10.1016/j.cis.2013.10.006 [in press].
[68] Khunova V, Kristof J, Kelnar I, Dybal J. The effect of halloysite modification combined with in situ matrix modifications on the structure and properties of polypropylene/halloysite nanocomposites. Express Polym Lett 2013;7:471–9.
[69] Abdullayev E, Joshi A, Wei W, Zhao Y, Lvov Y. Enlargement of halloysite clay nanotube lumen by selective etching of aluminum oxide. ACS Nano 2012;6:7216–26.
[70] White RD, Bavykin DV, Walsh FC. The stability of halloysite nanotubes in acidic and alkaline aqueous suspensions. Nanotechnology 2012;23, 065705/1-10.
[71] Joo Y, Sim JH, Jeon Y, Lee SU, Sohn D. Opening and blocking the inner-pores of halloysite. Chem Commun 2013;49:4519–21.
[72] Liu M, Li W, Rong J, Zhou C. Novel polymer nanocomposite hydrogel with natural clay nanotubes. Colloid Polym Sci 2012;290:895–905.
[73] Liu M, Zhang Y, Zhou C. Nanocomposites of halloysite and polylactide. Appl Clay Sci 2013;75–76:52–9.
[74] Rooj S, Das A, Thakur V, Mahaling RN, Bhowmick AK, Heinrich G. Preparation and properties of natural nanocomposites based on

natural rubber and naturally occurring halloysite nanotubes. Mater Des 2010;31:2151–6.
[75] Liu M, Guo B, Du M, Jia D. Drying induced aggregation of halloysite nanotubes in polyvinyl alcohol/halloysite nanotubes solution and its effect on properties of composite film. Appl Phys A 2007;88:391–5.
[76] Zhou WY, Guo B, Liu M, Liao R, Rabie ABM, Jia D. Poly(vinyl alcohol)/halloysite nanotubes bionanocomposite films: properties and in vitro osteoblasts and fibroblasts response. J Biomed Mater Res A 2010;93:1574–87.
[77] Ghebaur A, Garea SA, Iovu H. New polymer–halloysite hybrid materials – a potential controlled drug release system. Int J Pharm 2012;436:568–73.
[78] De Silva RT, Pasbakhsh P, Goh KL, Chai SP, Ismail H. Physico-chemical characterisation of chitosan/halloysite composite membranes. Polym Test 2013;32:265–71.
[79] Cavallaro G, Lazzara G, Milioto S. Dispersions of nanoclays of different shapes into aqueous and solid biopolymeric matrices. Extended physicochemical study. Langmuir 2011;27:1158–67.
[80] Cavallaro G, Donato DI, Lazzara G, Milioto S. Films of halloysite nanotubes sandwiched between two layers of biopolymer: from the morphology to the dielectric, thermal, transparency, and wettability properties. J Phys Chem C 2011;115:20491–8.
[81] Cavallaro G, Lisi R, Lazzara G, Milioto S. Polyethylene glycol/clay nanotubes composites. J Therm Anal Calorim 2013;112:383–9.
[82] He Y, Kong W, Wang W, Liu T, Liu Y, Gong Q, Gao J. Modified natural halloysite/potato starch composite films. Carbohydr Polym 2012;87:2706–11.
[83] Tang XG, Hou M, Zou J, Truss R. Poly(vinylidene fluoride)/halloysite nanotubes nanocomposites: the structures, properties, and tensile fracture behaviors. J Appl Polym Sci 2013;128:869–78.
[84] Cavallaro G, Gianguzza A, Lazzara G, Milioto S, Piazzese D. Alginate gel beads filled with halloysite nanotubes. Appl Clay Sci 2013;72:132–7.
[85] Du M, Guo B, Lei Y, Liu M, Jia D. Carboxylated butadiene–styrene rubber/halloysite nanotube nanocomposites: interfacial interaction and performance. Polymer 2008;49:4871–6.
[86] Ye Y, Chen H, Wu J, Ye L. High impact strength epoxy nanocomposites with natural nanotubes. Polymer 2007;48:6426–33.
[87] Huttunen-Saarivirta E, Vaganov GV, Yudin VE, Vuorinen J. Characterization and corrosion protection properties of epoxy powder coatings containing nanoclays. Prog Org Coat 2013;76:757–67.
[88] Albdiry MT, Yousif BF. Morphological structures and tribological performance of unsaturated polyester based untreated/silane-treated halloysite nanotubes. Mater Des 2013;48:68–76.
[89] Wang LP, Wang YP, Pei XW, Peng B. Synthesis of poly(methyl methacrylate)-b-poly(n-isopropylacrylamide) (PMMA-b-PNIPAM) amphiphilic diblock copolymer brushes on halloysite substrate via reverse ATRP. React Funct Polym 2008;68:649–55.
[90] Lin Y, Ng KM, Chan CM, Sun G, Wu J. High-impact polystyrene/halloysite nanocomposites prepared by emulsion polymerization using sodium dodecyl sulfate as surfactant. J Colloid Interface Sci 2011;358:423–9.
[91] Tierrablanca E, Romero-Garcia J, Roman P, Cruz-Silva R. Biomimetic polymerization of aniline using hematin supported on halloysite nanotubes. Appl Catal A 2010;381:267–73.
[92] Qi R, Guo R, Shen M, Cao X, Zhang L, Xu J, Yu J, Shi X. Electrospun poly(lactic-co-glycolic acid)/halloysite nanotube composite nanofibers for drug encapsulation and sustained release. J Mater Chem 2010;20:10622–9.
[93] Dong Y, Chaudhary D, Haroosh H, Bickford T. Development and characterisation of novel electrospun polylactic acid/tubular clay nanocomposites. J Mater Sci 2011;46:6148–53.
[94] Zhao Y, Wang S, Guo Q, Shen M, Shi X. Hemocompatibility of electrospun halloysite nanotube- and carbon nanotube-doped composite poly(lactic-co-glycolic acid) nanofibers. J Appl Polym Sci 2013;127:4825–32.
[95] Dong Y, Bickford T, Haroosh H, Lau KT, Takagi H. Multi-response analysis in the material characterisation of electrospun poly (lactic acid)/halloysite nanotube composite fibres based on taguchi design of experiments: fibre diameter, non-intercalation and nucleation effects. Appl Phys A 2013;112:747–57.
[96] Qi R, Cao X, Shen M, Guo R, Yu J, Shi X. Biocompatibility of electrospun halloysite nanotube-doped poly(lactic-co-glycolic acid) composite nanofibers. J Biomater Sci Polym Ed 2012;23:299–313.
[97] Liao RJ, Guo BC, Zhao JQ, Zhou WY. Electrospun polyvinyl alcohol/halloysite nanotubes composite nanofibers. In: The second international conference on advanced textile materials & manufacturing technology. 2010. p. 63–7.
[98] Lin TF [Master Thesis] Modifications of polypropylene fiber and FIBC model blend with halloysite nanotubes. Guangzhou, PR China: South China University of Technology; 2011, 59 pp. (in Chinese).
[99] Vergaro V, Abdullayev E, Lvov YM, Zeitoun A, Cingolani R, Rinaldi R, Leporatti S. Cytocompatibility and uptake of halloysite clay nanotubes. Biomacromolecules 2010;11:820–6.
[100] Konnova SA, Sharipova IR, Demina TA, Osin YN, Yarullina DR, Ilinskaya ON, Lvov YM, Fakhrullin RF. Biomimetic cell-mediated three-dimensional assembly of halloysite nanotubes. Chem Commun 2013;49:4208–10.
[101] Shchukin DG, Lamaka SV, Yasakau KA, Zheludkevich ML, Ferreira MGS, Mohwald H. Active anticorrosion coatings with halloysite nanocontainers. J Phys Chem C 2008;112:958–64.
[102] Zhai R, Zhang B, Wan Y, Li C, Wang J, Liu J. Chitosan–halloysite hybrid-nanotubes: horseradish peroxidase immobilization and applications in phenol removal. Chem Eng J 2013;214:304–9.
[103] Deen I, Pang X, Zhitomirsky I. Electrophoretic deposition of composite chitosan–halloysite nanotube-hydroxyapatite films. Colloids Surf A 2012;410:38–44.
[104] Deen I, Zhitomirsky I. Electrophoretic deposition of composite halloysite nanotube–hydroxyapatite–hyaluronic acid films. J Alloys Compd 2013;586:S531–4.
[105] Deng S, Zhang J, Ye L, Wu J. Toughening epoxies with halloysite nanotubes. Polymer 2008;49:5119–27.
[106] Liu M, Wu C, Jiao Y, Xiong S, Zhou C. Chitosan–halloysite nanotubes nanocomposite scaffolds for tissue engineering. J Mater Chem B 2013;1:2078–89.
[107] Lee KS, Chang YW. Thermal, mechanical, and rheological properties of poly(ε-caprolactone)/halloysite nanotube nanocomposites. J Appl Polym Sci 2013;128:2807–16.
[108] Pasbakhsh P, Ismail H, Fauzi MNA, Bakar AA. EPDM/modified halloysite nanocomposites. Appl Clay Sci 2010;48:405–13.
[109] Pasbakhsh P, Ismail H, Fauzi MNA, Bakar AA. Influence of maleic anhydride grafted ethylene propylene diene monomer (MAH-g-EPDM) on the properties of EPDM nanocomposites reinforced by halloysite nanotubes. Polym Test 2009;28:548–59.
[110] Prashantha K, Lecouvet B, Sclavons M, Lacrampe MF, Krawczak P. Poly(lactic acid)/halloysite nanotubes nanocomposites: structure, thermal, and mechanical properties as a function of halloysite treatment. J Appl Polym Sci 2013;128:1895–903.
[111] Rooj S, Das A, Heinrich G. Tube-like natural halloysite/fluoroelastomer nanocomposites with simultaneous enhanced mechanical, dynamic mechanical and thermal properties. Eur Polym J 2011;47:1746–55.
[112] Deng S, Zhang J, Ye L. Halloysite–epoxy nanocomposites with improved particle dispersion through ball mill homogenisation and chemical treatments. Compos Sci Technol 2009;69:2497–505.
[113] Lecouvet B, Sclavons M, Bourbigot S, Devaux J, Bailly C. Water-assisted extrusion as a novel processing route to prepare polypropylene/halloysite nanotube nanocomposites: structure and properties. Polymer 2011;52:4284–95.
[114] Jia ZX, Luo YF, Yang SY, Guo BC, Du ML, Jia DM. Morphology, interfacial interaction and properties of styrene–butadiene rubber/modified halloysite nanotube nanocomposites. Chin J Polym Sci 2009;27:857–64.
[115] Jia ZX, Luo YF, Yang SY, Du ML, Guo BC, Jia DM. Styrene–butadiene rubber/halloysite nanotubes composites modified by epoxidized natural rubber. J Nanosci Nanotechnol 2011;11:10958–62.
[116] Schmitt H, Prashantha K, Soulestin J, Lacrampe MF, Krawczak P. Preparation and properties of novel melt-blended halloysite nanotubes/wheat starch nanocomposites. Carbohydr Polym 2012;89:920–7.
[117] Liu M, Guo B, Du M, Zou Q, Jia D. Influence of hybrid fibrils of 2,5-bis(2-benzoxazolyl) thiophene and halloysite nanotubes on the crystallization behaviour of polypropylene. J Phys D 2009;42:075306/1-9.
[118] Liu M, Guo B, Lei Y, Du M, Jia D. Benzothiazole sulfide compatibilized polypropylene/halloysite nanotubes composites. Appl Surf Sci 2009;255:4961–9.
[119] Guo B, Chen F, Lei Y, Jia D. Tubular clay composites with high strength and transparency. J Macromol Sci Phys 2010;49:111–21.
[120] Guo B, Chen F, Lei Y, Liu X, Wan J, Jia D. Styrene–butadiene rubber/halloysite nanotubes nanocomposites modified by sorbic acid. Appl Surf Sci 2009;255:7329–36.
[121] Guo B, Lei Y, Chen F, Liu X, Du M, Jia D. Styrene–butadiene rubber/halloysite nanotubes nanocomposites modified by methacrylic acid. Appl Surf Sci 2008;255:2715–22.

[122] Liu M, Jia Z, Liu F, Jia D, Guo B. Tailoring the wettability of polypropylene surfaces with halloysite nanotubes. J Colloid Interface Sci 2010;350:186–93.
[123] Liu M, Guo B, Du M, Chen F, Jia D. Halloysite nanotubes as a novel beta-nucleating agent for isotactic polypropylene. Polymer 2009;50:3022–30.
[124] Guo B, Zou Q, Lei Y, Du M, Liu M, Jia D. Crystallization behavior of polyamide 6/halloysite nanotubes nanocomposites. Thermochim Acta 2009;484:48–56.
[125] Attia NF, Hassan MA, Nour MA, Geckeler KE. Flame-retardant materials: synergistic effect of halloysite nanotubes on the flammability properties of acrylonitrile–butadiene–styrene composites. Polym Int 2013, http://dx.doi.org/10.1002/pi.4653.
[126] Lecouvet B, Sclavons M, Bourbigot S, Bailly C. Thermal and flammability properties of polyethersulfone/halloysite nanocomposites prepared by melt compounding. Polym Degrad Stab 2013;98:1993–2004.
[127] Rybinski P, Janowska G. Influence synergetic effect of halloysite nanotubes and halogen-free flame-retardants on properties nitrile rubber composites. Thermochim Acta 2013;557:24–30.
[128] Nakamura R, Netravali AN, Morgan AB, Nyden MR, Gilman JW. Effect of halloysite nanotubes on mechanical properties and flammability of soy protein based green composites. Fire Mater 2013;37:75–90.
[129] Fix D, Andreeva DV, Lvov YM, Shchukin DG, Möhwald H. Application of inhibitor-loaded halloysite nanotubes in active anti-corrosive coatings. Adv Funct Mater 2009;19:1720–7.
[130] Abdullayev E, Price R, Shchukin D, Lvov Y. Halloysite tubes as nanocontainers for anticorrosion coating with benzotriazole. ACS Appl Mater Interfaces 2009;1:1437–43.
[131] Abdullayev E, Abbasov V, Tursunbayeva A, Portnov V, Ibrahimov H, Mukhtarova G, Lvov Y. Self-healing coatings based on halloysite clay polymer composites for protection of copper alloys. ACS Appl Mater Interfaces 2013;5:4464–71.
[132] Haroosh H, Dong Y, Chaudhary D, Ingram G, Yusa SI. Electrospun PLA: PCL composites embedded with unmodified and 3-aminopropyltriethoxysilane (ASP) modified halloysite nanotubes (HNT). Appl Phys A 2013;110:433–42.
[133] Levis SR, Deasy PB. Characterisation of halloysite for use as a microtubular drug delivery system. Int J Pharm 2002;243:125–34.
[134] Viseras M, Aguzzi C, Cerezo P, Cultrone G, Viseras C. Supramolecular structure of 5-aminosalycilic acid/halloysite composites. J Microencapsul 2008;26:279–86.
[135] Aguzzi C, Viseras C, Cerezo P, Salcedo I, Sanchez-Espejo R, Valenzuela C. Release kinetics of 5-aminosalicylic acid from halloysite. Colloids Surf B 2013;105:75–80.
[136] Veerabadran NG, Price RR, Lvov YM. Clay nanotubes for encapsulation and sustained release of drugs. Nano 2007;02:115–20.
[137] Forsgren J, Jämstorp E, Bredenberg S, Engqvist H, Strømme MA. ceramic drug delivery vehicle for oral administration of highly potent opioids. J Pharm Sci 2010;99:219–26.
[138] Levis SR, Deasy PB. Use of coated microtubular halloysite for the sustained release of diltiazem hydrochloride and propranolol hydrochloride. Int J Pharm 2003;253:145–57.
[139] Abdullayev E, Lvov Y. Halloysite clay nanotubes as a ceramic "Skeleton" for functional biopolymer composites with sustained drug release. J Mater Chem B 2013;1:2894–903.
[140] Shi YF, Tian Z, Zhang Y, Shen HB, Jia NQ. Functionalized halloysite nanotube-based carrier for intracellular delivery of antisense oligonucleotides. Nanoscale Res Lett 2011;6, 608/1-7.
[141] Hughes AD, King MR. Use of naturally occurring halloysite nanotubes for enhanced capture of flowing cells. Langmuir 2010;26:12155–64.
[142] Wei W, Abdullayev E, Hollister A, Mills D, Lvov YM. Clay nanotube/poly(methyl methacrylate) bone cement composites with sustained antibiotic release. Macromol Mater Eng 2012;297:645–53.
[143] Luo BH, Hsu CE, Li JH, Zhao LF, Liu MX, Wang XY, Zhou CR. Nano-composite of poly(L-lactide) and halloysite nanotubes surface-grafted with L-lactide oligomer under microwave irradiation. J Biomed Nanotechnol 2013;9:649–58.
[144] Suh YJ, Kil DS, Chung KS, Abdullayev E, Lvov YM, Mongayt D. Natural nanocontainer for the controlled delivery of glycerol as a moisturizing agent. J Nanosci Nanotechnol 2011;11:661–5.
[145] Luo P, Zhang JS, Zhang B, Wang JH, Zhao YF, Liu JD. Preparation and characterization of silane coupling agent modified halloysite for Cr(VI) removal. Ind Eng Chem Res 2011;50:10246–52.
[146] Zhang Y, Chen Y, Zhang H, Zhang B, Liu J. Potent antibacterial activity of a novel silver nanoparticle–halloysite nanotube nanocomposite powder. J Inorg Biochem 2013;118:59–64.
[147] Ning NY, Yin QJ, Luo F, Zhang Q, Du R, Fu Q. Crystallization behavior and mechanical properties of polypropylene/halloysite composites. Polymer 2007;48:7374–84.
[148] Lecouvet B, Bourbigot S, Sclavons M, Bailly C. Kinetics of the thermal and thermo-oxidative degradation of polypropylene/halloysite nanocomposites. Polym Degrad Stab 2012;97:1745–54.
[149] Ismail H, Salleh SZ, Ahmad Z. Fatigue and hysteresis behavior of halloysite nanotubes-filled natural rubber (SMR L and ENR 50) nanocomposites. J Appl Polym Sci 2013;127:3047–52.
[150] Ismail H, Shaari SM. Curing characteristics, tensile properties and morphology of palm ash/halloysite nanotubes/ethylene-propylene-diene monomer (EPDM) hybrid composites. Polym Test 2010;29:872–8.
[151] Shamsi MH, Geckele KE. The first biopolymer-wrapped non-carbon nanotubes. Nanotechnology 2008;19, 075604/1-5.